frontiers | Frontiers in Earth Science

TYPE Original Research
PUBLISHED 25 January 2023
DOI 10.3389/feart.2022.1086298

OPEN ACCESS

EDITED BY
Ruoyu Sun,
Tianjin University, China

REVIEWED BY
Jian Chen,
Anhui University of Science and Technology, China
Xianfeng Tan,
Chongqing University of Science and Technology, China

*CORRESPONDENCE
Zhihui Zhang,
zhzhihui@sdust.edu.cn

SPECIALTY SECTION
This article was submitted to Geochemistry, a section of the journal Frontiers in Earth Science

RECEIVED 01 November 2022
ACCEPTED 28 November 2022
PUBLISHED 25 January 2023

CITATION
Lv D, Shen Y, van Loon AJT, Raji M, Zhang Z, Song G, Ren Z, Wang Y and Wang D (2023), Sequence stratigraphy of the Middle Jurassic Yan'an Formation (NE Ordos Basin, China), relationship with climate conditions and basin evolution, and coal maceral's characteristics. *Front. Earth Sci.* 10:1086298. doi: 10.3389/feart.2022.1086298

Sequence stratigraphy of the Middle Jurassic Yan'an Formation (NE Ordos Basin, China), relationship with climate conditions and basin evolution, and coal maceral's characteristics

Dawei Lv[1,2], Yangyang Shen[1], A. J. Tom van Loon[1], Munira Raji[3], Zhihui Zhang[1]*, Guangzeng Song[4], Zhouhe Ren[4], Yujia Wang[1] and Dongdong Wang[1]

[1]Shandong Provincial Key Laboratory of Depositional Mineralization and Sedimentary Minerals, College of Earth Sciences and Engineering, Shandong University of Science and Technology, Qingdao, China, [2]Laboratory for Marine Mineral Resources, Qingdao National Laboratory for Marine Science and Technology, Qingdao, China, [3]Sustainable Earth Institute, University of Plymouth, Devon, United Kingdom, [4]School of Water Conversancy and Environment, University of Jinan, Jinan, China

The Yan'an Formation of the Ordos Basin in North China is among the largest and most extensively studied Jurassic coal reservoirs in the world. The lacustrine Yan'an Formation was investigated near Dongsheng (Ordos Basin, China) in its sequence-stratigraphic context, to understand the factors that controlled the peat accumulation and the cyclicity in the coal-bearing strata. Nine facies, grouped into two facies associations, jointly composed two third-order sequences. These represent lowstand system tracts, extended (lacustrine) system tracts and highstand system tracts. The sequence stratigraphic framework could be established on the basis of correlations of cores and logging from several wells. It appears that the coal development was controlled partly by fluctuations of the lake level. The sequence development controlled the vertical distribution of the coal seams, which mainly developed during extended lacustrine system tracts (= during transgressive stages of the lake) and the early stage of highstand system tracts. Sequence stratigraphy and maceral analysis indicate that basin subsidence and climate were the main controlling factors for the development of the coal seams and the coal-bearing succession. A generic model was established to show the lateral and vertical distribution of coal seams in the large, subsiding lacustrine coal basin with no significant folding or faulting. Special attention is paid to the changing climate conditions. The findings are considered to help deepen the theory of coal formation; they will also help increase the efficacy of coal exploitation in basins such as the Ordos Basin.

KEYWORDS

Yan'an Formation, Jurassic, Coal formation, Macerals, Ordos Basin, Sequence stratigraphy

1 Introduction

Cycles in coal measures must be ascribed to phases in their development under conditions of regular alternation (Ward, 1984; Catuneanu, 2006; Catuneanu, 2020). The study of such cycles is consequently an important tool for the reconstruction of the environmental changes under which the coal was formed (Dai and Finkelman, 2018; Fielding, 2021). Moreover, a good insight into these changing environmental conditions helps not only to compare the developments in different coal-bearing successions in the same basin, but also can facilitate exploration for economically exploitable coal fields (Biswas et al., 2021).

Cyclic patterns, including those of coal measures, have always been a hot topic in geology and particularly sedimentology, with special application to coal geology. Analyses of numerous coal measures (Klein and Willard, 1989; Klein, 1990; Calder, 1994; Cameron et al., 1994) have led to the conclusion that climate is the main factor controlling these cycles (Calder, 1994; Holz et al., 2002). We here put forward sound arguments, however, that implies that quiet but somewhat irregular basin subsidence must have played an at least equally important role in the coal cycles (Miall, 2013). The irregular subsidence must, in addition to the climate, also have played an important role in the cyclical occurrences of specific coal types, as present in the various system tracts. Many more factors influence the formation of different types of coal, particularly tectonics, glacially-induced sea-level changes, sediment supply, and climate (Klein and Willard, 1989), but the role of more or less continuous basin subsidence has largely been neglected in studies varied out during the past few decades, although some studies recognized and even emphasized the importance of this aspect (Zhao et al., 2022).

The cycles of coal measures developed in tectonically quiet lacustrine basins obviously differ from those in coastal areas, as more sediment tends to be supplied, and as eustatic sea-level fluctuations commonly have no influence. These differences are also reflected in the lithology: whereas limestones tend to be common in coastal coal measures, they are very rare in lacustrine equivalents.

These differences are important for the present study, because the focus is here on coal seams in the lacustrine Yan'an Formation, which forms a Jurassic succession in the Ordos Basin. Although the Yan'an Formation and its coal measures have attracted attention already for a long time (Johnson et al., 1989; Jiao et al., 2016; Wang et al., 2018), still many questions have to be answered, such as 1) what types of coal-measure cycles can be distinguished in lacustrine successions such as the one under study here? 2) What system tracts are they formed in? 3) What are the differences in the coal macerals of the various coal types? And 4) what are the main factors controlling the coal formation and the cyclicity in the coal measures developed in large lacustrine basins with a relatively stable tectonic setting?

2 Study area and geological setting

The cyclical coal measures under study here, forming part of the Jurassic Yan'an Formation, developed in the overall lacustrine setting of the Ordos Basin, and developed in environments ranging from a meandering river to a lacustrine delta. The study area was tectonically stable at the time, and sediment was supplied from nearby source areas (Chen et al., 2022).

The Ordos Basin, which covers an area of about 250,000 km^2, is well known for its vast energy resources (Yao et al., 2013; Zhang et al., 2017; Yang and Van Loon, 2022), among which coal is abundant (Dai and Finkelman, 2018; Zhang et al., 2021a; Li et al., 2021b). The area under study in the present contribution is the Dongsheng Coalfield near Ordos City, Inner Mongolia, which is located in the north-eastern margin of the basin (Figure 1A). The Yan'an Formation is well developed here and is exposed in an area of some 2,000 km^2; it reaches a thickness of 133–279 m.

The development of the Yan'an Formation must, obviously, be understood in the context of the basin's history. The basin originated in the Mesoproterozoic but developed a thick sedimentary succession since the Early Paleozoic (Akhtar et al., 2017). The surroundings of the basin have been tectonically strongly active, and Mesozoic and Cenozoic activity resulted in a complex orogenic zone around the basin (Liu et al., 2021). In contrast, the interior remained relatively stable, although uplift, subsidence, and some folding have taken place (Johnson et al., 1989; Liu et al., 2021; Wang et al., 2022; Zhang et al., 2022).

The study area, which covers part of the Dongsheng Coalfield, is situated in the area around Tongjiangchuan near Ordos City and the exposed rocks consist mainly of Mesozoic sediments (Figure 1B). The overall more or less flat-lying sediments in the Dongsheng Coalfield form a simple homocline with a gentle dip of 1–3° toward the SE. A regional unconformity is present between the Late Triassic Yanchang Formation and the Middle Jurassic (Figure 1C), which consists of the Yan'an Fm. and the overlying Zhiluo Fm. (Ma et al., 2007; Zhang Q. et al., 2022).

The Yan'an Formation is the main coal-bearing unit (Figure 1C). It consists mainly of sandstone and mudstone, and the intercalated coal seams are divided into six main units (Figure 1C), coded from top to bottom as 2-2, 3-1, 4-1,

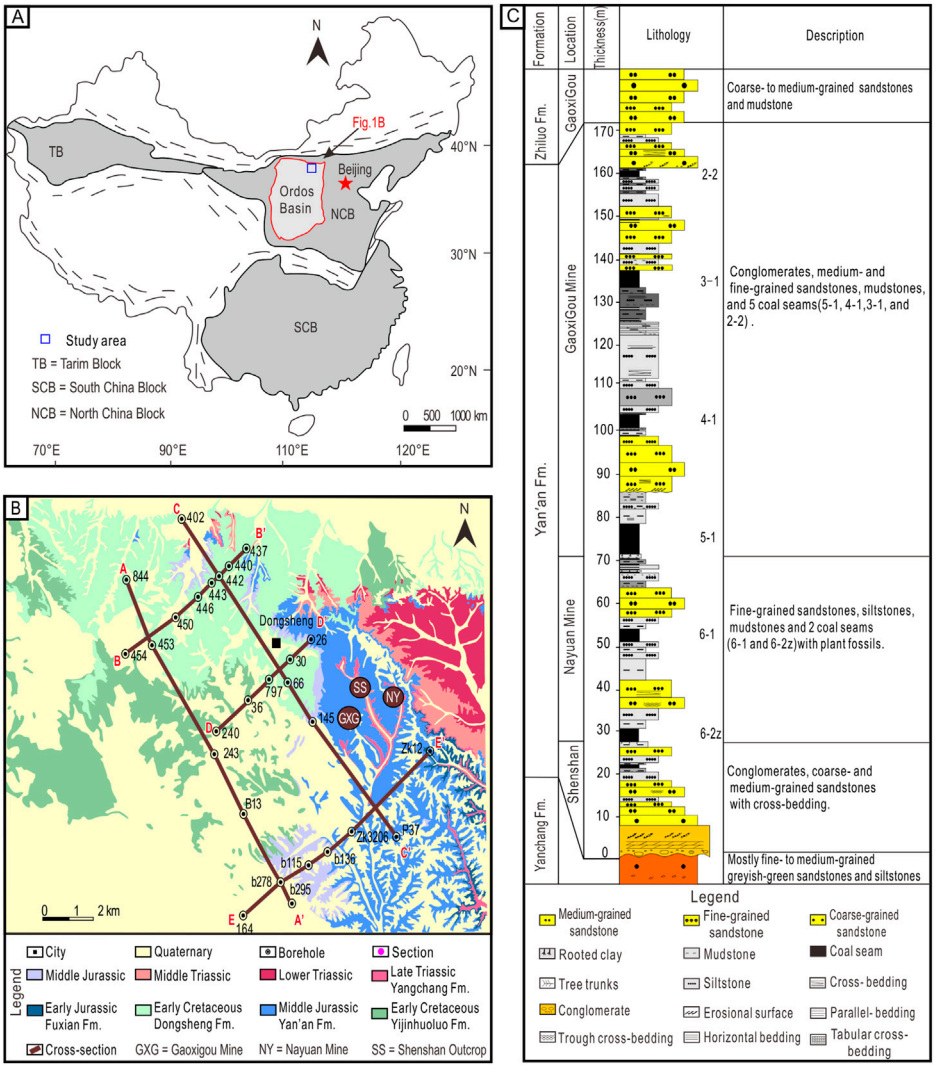

FIGURE 1
(A) Location of the Ordos Basin in China, and location of the study area within the Ordos Basin. **(B)** Borehole map of the study area. **(C)** Composite sedimentary log of the Yan'an Fm., with top part of the underlying Yanchang Fm. and basal part of the overlying Zhiluo Fm.

5-1, 6-1, and 6-2z (Li et al., 1992). The six coal seams are laterally continuous in the Dongsheng Coalfield. The Yan'an Formation is exposed at open pit mines in the coalfield, which allow a complete succession of the Yan'an Formation to be constructed. Moreover, an extensive network of boreholes drilled across the coalfield for exploration purposes facilitates stratigraphic correlation of the Yan'an Formation by the six coal seams.

3 Methods

Much is already known about the lithology of the Yan'an Fm., so the lithofacies are mentioned only shortly (Section 3.1). New information was obtained mostly by analysis of the sequence stratigraphy (Section 3.2) and the coal petrology (Section 3.3).

3.1 Lithofacies analysis

The various lithofacies and their associations have been investigated in numerous earlier studies (Miall, 1977; Wescott and Ethridge, 1980; Nemec and Steel, 1988; Mjos and Prestholm, 1993; Hwang et al., 1995; Junnila and Young, 1995; Kneller and Branney, 1995; Miall, 1996; Krassay et al., 2000; Boyd et al., 2006; Ielpi, 2012; Wang et al., 2020) and we refer here to these studies. We carried out some additional lithofacies analyses of the coal

measures (see Section 4.1) in order to identify cycles, with the objective to deepen the understanding of the sedimentary environment of these coal-measure cycles (Diesel and Wolff-Fischer, 1986; Diessel and Gammidge, 1998).

3.2 Sequence stratigraphy

The sequence-stratigraphically important levels were identified following the method described in detail by Catuneanu (2019). Initial (lake) flooding surfaces (IFS) and maximum (lake) flooding surfaces (MFS) needed most attention. IFS were identified on the basis of the transition of the stacking pattern in the succession from progradational to retrogradational, indicating that the lake changed from regression to transgression (Catuneanu, 2006; Li et al., 2018; Wang et al., 2020). MFS, in contrast, were recognized because of the change from retrogradation to aggradation or even progradation (Li et al., 2018; Li et al., 2020; Li et al., 2021a), marking the end of a lacustrine transgression with a change of the lake shoreline to regression (Catuneanu, 2006; Li et al., 2018; Wang et al., 2020). It can thus be deduced that, when an MFS was formed, the lake area had its largest extent, and that the sedimentation rate was lower than the rate at which the accommodation space increased. This led to the deposition of a condensed layer.

In order to understand the sequence-stratigraphic framework of the Yan'an Formation in the study area, several boreholes were selected for such an analysis. As will be detailed in Section 4.2.3, the Yan'an Formation consists of two third-order sequences, which are characterized by a specific vertical arrangement of lithofacies associations. The various system tracts with different lithofacies associations were therefore determined, and the evolution of the depositional environment was reconstructed on the basis of core analysis from a single well and correlation of the thus obtained data with other wells (Souza et al., 2021).

3.3 Coal-petrology analysis

Coal samples were collected from the two coal mines (Figure 1B): the randomly selected samples from seams 2-2, 3-1, 4-1, and 5-1 were collected from the Gaoxigou mine, and those from seams 6-1 and 6-2z were collected from the Nayuan mine. Moreover, 176 samples were collected from all coal seams at 10-cm sampling intervals for maceral analysis. The macerals were analyzed in order to obtain insight into the diagenetic conditions under which the coals had formed, and into the coal types.

The coal samples were air-dried, crushed to a maximum grain size of 2 mm, and prepared as polished epoxy-bound pellets for the analyses. The macerals and inertinite reflectance of all samples were determined at the Shandong Provincial Key Laboratory of Depositional Mineralization & Sedimentary Minerals using a Zeiss Axio Scope A1 reflected-light microscope equipped with an MSP UV-VIS2000 spectrophotometer. The petrological composition was determined for each sample by counting at least 500 points and subsequently classified (Sýkorová et al., 2005); the maceral classification and terminology applied in the present contribution are based on Taylor et al. (1998) and ICCP 1994 (ICCP (International, 1998). The thus counted maceral and mineral composition was subsequently converted into percentages (by volume) for each maceral and mineral.

Commonly used coal parameters include the Gelation Index (GI) and the Texture Preservation Index (TPI) (Diessel, 1986). The GI refers to the ratio between macerals with and without gelatinization in the coal: GI = (vitrinite + megasome)/(fusinite + semifusinite + inertodetrinite); this indicates the degree of gelatinization of coal-forming plant residues (Diessel, 1992a; Diessel, 1992b; Jiu et al., 2021; Akinyemi et al., 2022). The TPI refers to the ratio of textured and untextured maceral components in the vitrinite and inertinite: TPI = (telinite + telocollinite + fusinite + semifusinite)/(desmocollinite + megasome + inertodettinite); TPI thus indicates the degree of fragmentation of plant tissues and the ratio of xylophytes in the coal-forming plants (Diessel, 1992a; Diessel, 1992b; Lu et al., 2017; Jiu et al., 2021).

A GI index over 1 reflects a relatively wet climate and the probable presence of a peat swamp covered with relatively deep water (Teichmüller, 1989); a GI index of less than 1 reflects a relatively dry climate with the probable presence of a peat swamp covered with shallow water (Diessel et al., 2000a; Diessel et al., 2000b; Akinyemi et al., 2022). A TPI index of over 1 indicates that the coal-forming plants were dominated by xylophytes with good structural preservation (Flores, 2002; Guo et al., 2018); a TPI index of less than 1 indicates that the coal-forming plants were dominated by herbaceous plants (Harvey and Dillon, 1985; Diesel and Wolff-Fischer, 1986).

4 Results

The origin of the coal seams can be understood only if their sedimentary context is understood. It is therefore necessary to pay attention here first to the various facies and facies associations in the sections under study (Section 4.1). Subsequently, these facies and their associations will be dealt with in their sequence-stratigraphic context (Section 4.2); when the context of the coal seams is clear, the analyses of the coal petrology will be dealt with (Section 4.3). This will, finally, result in the relationship between facies and coal development (Section 4.4).

TABLE 1 Main lithofacies of the Yan'an Formation in the Dongsheng Coalfield of the Ordos Basin.

Lithofacies code	Lithofacies	Description	Interpretation
Gp	Fining-upward graded bedding, quartzose sandy conglomerate	The gravel is mainly composed of quartz, mainly grayish white and grayish yellow, with high hardness, poor sorting, medium roundness, and no plant fossils, tabula-bedding, parallel bedding, upward-fining trend, and multiple stages of repeated development	Meandering river channel, delta distributary channel (Wescott and Ethridge, 1980; Miall, 1996)
Sp	Tabular cross-bedded gravel-bearing coarse-grained sandstones	Generally grayish white, poorly sorted and rounded, containing feldspar and quartz, there are many gravel particles in the coarse sandstone layer, cross-bedding is developed in the sandstone layer, hydrodynamic conditions are strong, and no plant fossils are found	Delta distributary channel, meandering river channel (Nemec and Steel, 1988; Ielpi, 2012)
St	Trough cross-bedded and horizontally laminated medium-grained sandstones	Gray or gray-black, medium sorting and grinding, medium quartz content, visible horizontal bedding, and coal line development. Trough bedding and lenticular limestone nodules are developed at the bottom of the Yan'an Formation	Delta distributary channel, meander channel (Hwang et al., 1995; Ielpi, 2012)
Sr	Cross-bedding fine-grained sandstone	Gray or gray-white, well sorted and rounded, high content of feldspar, which can be seen as obvious cross-bedding. Plant detrital fossils are unevenly distributed, and a layer of sandstone and a layer of organic matter are alternately arranged	Meandering river channel, delta distributary channel (Mjos and Prestholm, 1993)
Sh	Horizontally laminated siltstones	Gray or grayish-white, grayish black, large thickness, good sorting and rounding, more feldspar debris, less quartz content, containing crumby marl lens (foaming by dropping hydrochloric acid). Wavy bedding and horizontal bedding are developed	Floodplains, mouth bars, and natural levee of meandering river (Mjos and Prestholm, 1993; Junnila and Young, 1995; Krassay et al., 2000)
Fm	Gray, horizontally laminated mudstone	Gray, grayish black and grayish white, the surface is seriously weathered, the fracture is greasy luster, most of them develop horizontal bedding, and there are a large number of plant fossils (plant debris rhizomes).Some mudstones contain silty mudstone, argillaceous siltstone, coal line and marl lens	Peat bogs, Floodplains, natural levee of meandering rivers, wash land (Reading, 1996)
Fl	Rooted mudstone	The rocks are mostly distributed in the lower part of the coal seam, the color is gray or gray black, the bedding is not obvious, and the plant rhizome fossils are mostly perpendicular or oblique to the layer	Peat mire (Diessel, 1992b)
C	Coal	Light black, black, thin or massive; banded structure, and the weathered surface is powder; the cleavage surface is glassy. Plant stem and leaf fossils can be seen, which is developed on a large scale in the Yan'an Formation	Peat mire, flood plain (Diessel, 1992a; Diessel, 1992b; Diessel et al., 2000a; Diessel et al., 2000b)
FI	Interbedded gray sandstone and gray-white mudstone	Grayish-white, thinly laminated, medium sorting and rounding, ranges from centimeters to meters in thickness, sandstone alternates with mudstone, heavily weathered and develops horizontal laminated, mudstone contains coal line, fossilized plant stems and leaves is distributed in layers	Peat mire, flood plain, washland (Miall, 1996)

4.1 Facies and facies associations

It appears that nine lithofacies can be distinguished in the Yan'an Formation within the Dongsheng Coalfield (Supplementary Figure S1; Table 1), including some facies that contain coal, coaly material and/or plant fossils (Supplementary Figure S1). These lithofacies can be grouped into two lithofacies associations (FA1 and FA2) (Table 2).

4.1.1 Facies and depositional environment of association FA1

Seven lithofacies are grouped in this association because the facies are stacked upon each other and jointly show a fining upward trend (Supplementary Figure S2A). The nine lithofacies of FA1 are characterized by, respectively, quartzose sandy conglomerates that show distinct scouring and that are occasionally discontinuous (lithofacies Gp), tabular cross-

TABLE 2 Facies associations of the Yan'an Formation in the Dongsheng Coalfield of the Ordos Basin.

Facies associations	Constituent facies	Depositional environment
FA1	Gp, Sp, St, Sr, Sh, C, Fm	Meandering river
FA2	St, Sr, Sh, FI, Fr, C, Fm	Lacustrine delta

bedded gravel-bearing coarse-grained sandstones (Sp), trough cross-bedded and horizontally laminated medium-grained sandstones (St), cross-bedded fine-grained sandstone (Sr), horizontally laminated siltstones (Sh), coal or coaly beds (C), and gray, horizontally laminated mudstones (Fm) (Supplementary Figure S2A). Lithofacies Gp and Sp, which form the lowest part of FA1, consist of moderately sorted and poorly rounded particles. Lithofacies St and Sr have, in contrast, well sorted and rounded sand grains. Facies Sh and Fm overly Sr and contain fairly frequent plant fossils. Lithofacies C is about 0.3–0.4 m thick and forms the top of FA1.

The interpretation of these lithofacies is simple, as they have been described frequently in studies from successions ranging from the Carboniferous to the Neogene. They are characteristic of a meandering river system. Lithofacies Gp is common in the channels of a meandering river and in the distributary channels of a delta (Lowe, 1982). Lithofacies Sp typically suggests an environment with high-energy currents. Lithofacies St and Sr are characteristic of point bars. The plant fossils indicate weak currents and settling from suspension, which is common for a flood plain. Consequently, all lithofacies fit in the system of a meandering river depositional environment.

4.1.2 Facies and depositional environment of association FA2

The seven lithofacies of this association are characterized, respectively, by trough and tabular cross-bedded and horizontally laminated medium-grained well-sorted sandstones with rounded grains (St), trough and tabular cross-bedded fine-grained well-sorted sandstones with rounded sand grains (Sr), horizontally laminated siltstones (Sh), gray, horizontally laminated mudstones (Fm), intercalated gray sandstones and grayish-white mudstones (FI) with plant fossils, rooted clay (Fr), and coal beds (C) (Supplementary Figure S2B). Compared with association FA1, the grain size is smaller. Facies Fm and C, which form the lowermost facies of FA2, contain plant fossils. These facies are overlain by facies Sh, which contain a number of thin-layered coal seams in their top parts. The topmost facies of FA2 are facies Fm and C. Facies C is locally intercalated within rooted clay.

The interpretation of the depositional environment of association FA2 is a lacustrine delta. Facies Fm and C with their numerous plant fossils indicate low-energy conditions well comparable to those of a prodelta, deep-marine or lacustrine environment (Reading, 1996; Diessel et al., 2000a; Diessel et al., 2000b). The horizontally bedded facies Sh has been interpreted by Miall (1996) as characteristic of an interdistributary bay. The combination with facies Sr suggests deposition as a mouth bar (Mjos and Prestholm, 1993). Facies St and Sr with their tabular and trough cross-bedding and scours, represent distributary channels (Mjos and Prestholm, 1993; Hwang et al., 1995; Ielpi, 2012). Facies C and Fm at the top of the association indicate a peat-bog environment (Diessel, 1992a; Diessel et al., 2000b; Edress et al., 2021; Guatame and Rincón, 2021). The vertical fine-grained succession of association FA2 thus represents a lacustrine deltaic environment.

4.2 Sequence stratigraphy

The sediments under study have been analyzed for their sequence-stratigraphic aspects. The results are presented in the following sections for the sequence boundaries (Section 4.2.1) and the boundaries of the system tracts (Section 4.2.2). This results in a sequence-stratigraphic framework (Section 4.2.3), representing two third-order sequences (S-1 and S-2) that are each dealt with in Sections 4.2.3.1, 4.2.3.2, respectively.

4.2.1 Sequence boundaries

The sequence boundaries of the Yan'an Formation in the study area are represented by regional unconformities and abrupt changes of the facies, due to the (also abruptly changing) depositional conditions (Supplementary Figure S3). It appears that three such unconformities can be distinguished (from bottom to top sequence boundaries SB1 to SB3), thus bounding (see Section 4.3.2) two complete third-order sequences (S-1 and S-2).

The lowermost sequence boundary (SB1) is the unconformity that forms the boundary between the Yan'an Formation and the underlying Yanchang Formation. This sequence boundary forms the base of sequence S-1 (Supplementary Figure S3A), which starts with facies Gp and Sp. The quartz grains are oriented more or less horizontally, parallel lamination and cross-bedding occur frequently, and erosion by the currents in the river is distinctly present (Supplementary Figure S1A). Sequence S-1 is bounded at its top by sequence boundary SB2. The transition from the coarse top of sequence S-1 to sequence S-2 is lithologically abrupt: the lower part of sequence S-2 is dominated by silty mudstones. The upper part of sequence S-2 gradually changes into coarse and thick sandstones. The channel erosion is distinct (Supplementary

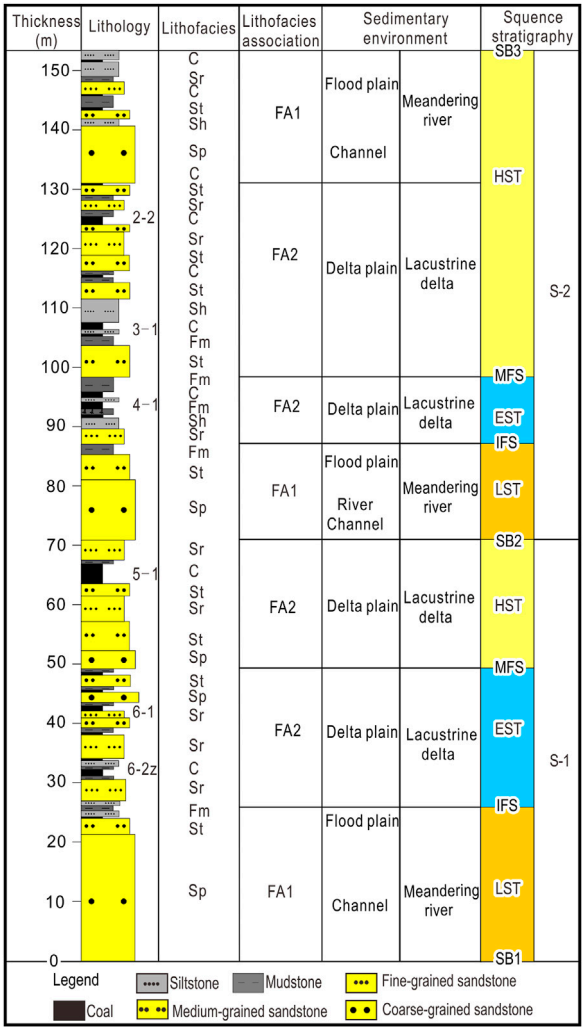

FIGURE 2
Lithology, lithofacies, depositional environment and sequence stratigraphy as determined for borehole 30. See Figure 1B for well location.

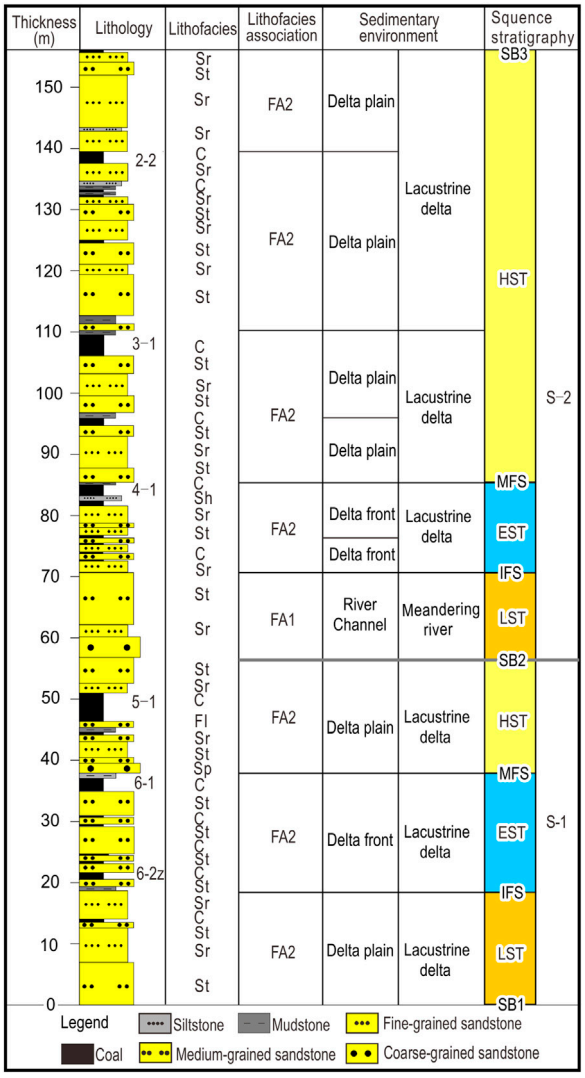

FIGURE 3
Lithology, lithofacies, depositional environment and sequence stratigraphy as determined for borehole 243. See Figure 1B for well location.

Figure S3C). Sequence S-2 is bounded at the top by sequence boundary SB3, which is the unconformity between the Yan'an Formation and the overlying Zhiluo Formation. This unconformity represents an incised valley (Supplementary Figure S3B).

4.2.2 System tract boundaries

System tract boundaries are controlled by changes of the base-level (Van Wagoner et al., 1988), and are represented by initial flooding surfaces (IFS) and maximum flooding surface (MFS).

IFS can be identified because of the transition of the succession from progradational to retro gradational (Supplementary Figure S3D), which indicates that a (here: lacustrine) regression changed into a transgression (Catuneanu, 2006; Catuneanu et al., 2009; Li et al., 2018). This development results in a distinct lithofacies change (Figures 2, 3). The beginning of the lacustrine transgression is reflected by a lower part of the succession that commonly consists of fluvial sandstones (Supplementary Figure S3D) and an upper part that is dominated by deltaic sand- and mudstones.

The MFS are recognized by their change from retrogradation to progradation (Supplementary Figure S3E), marked by a lake shoreline trajectory transition from an extended (lake) system tract (EST) to a highstand system tract (HST) (Shanley and McCabe, 1994; Plint et al., 2001; Catuneanu, 2006). The lower part of the MFS of the Yan'an Formation consists of mudstones and a coal seam, whereas the upper part consists of sandstones

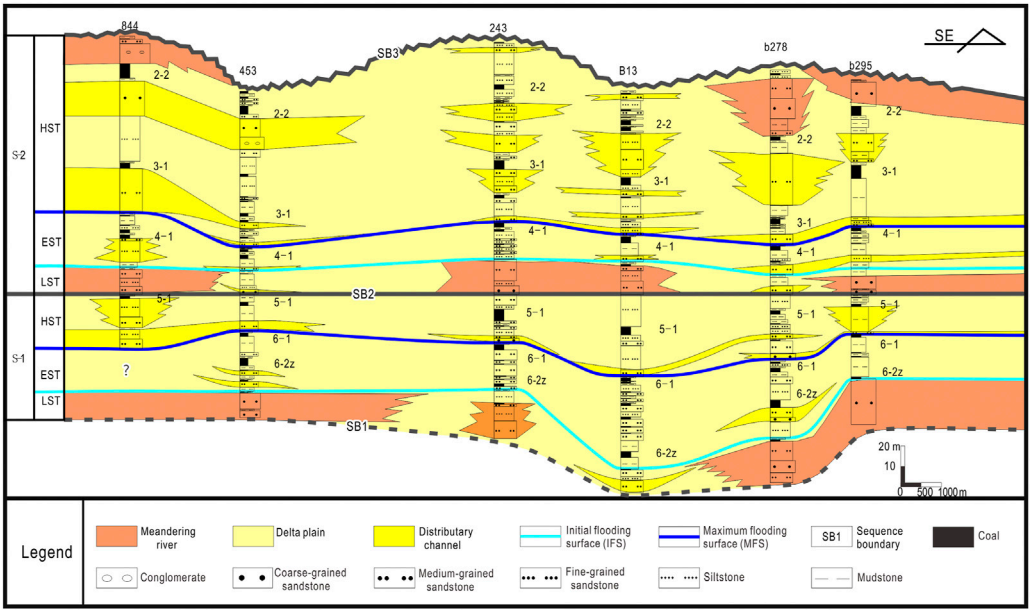

FIGURE 4
NW-SE cross-section (A-A′) through the Yan'an Formation, showing lithofacies, interpreted depositional environments (including coal seams) and sequence-stratigraphic data. The intraformational sequence boundary SB2 is taken as horizontal. See Figure 1B for location of the cross-section.

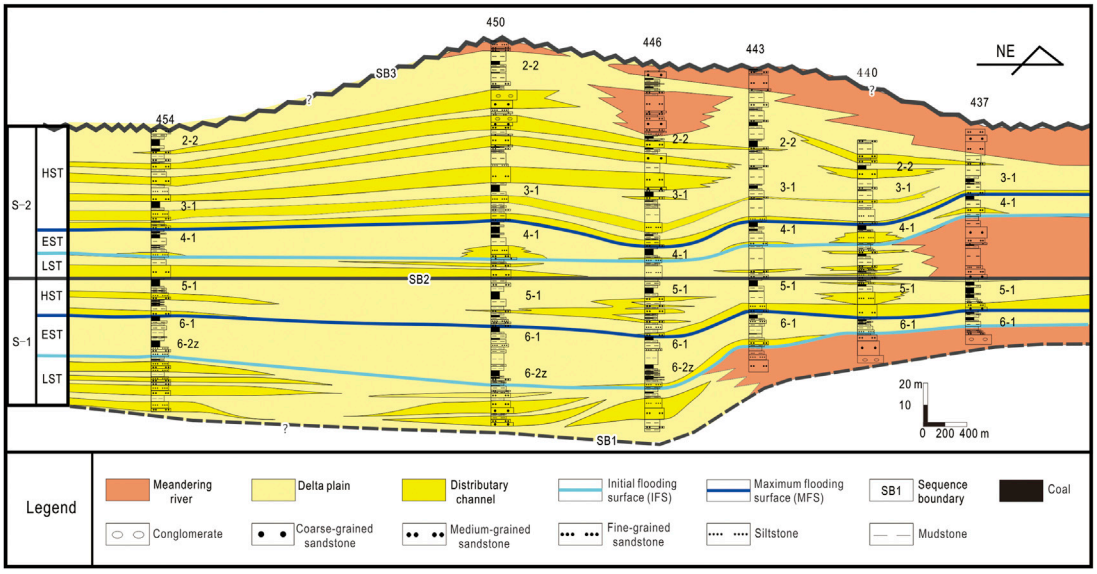

FIGURE 5
NE-SW cross-section (B-B′) through the Yan'an Formation, showing lithofacies, interpreted depositional environments (including coal seams) and sequence-stratigraphic data. The intraformational sequence boundary SB2 is taken as horizontal. See Figure 1B for location of the cross-section.

(Supplementary Figure S3E). The MFS is often accompanied by a condensed layer that represents the end of the lake transgression (Figures 2, 3).

4.2.3 Sequence stratigraphic framework

Based on the analysis of the sequence boundaries, the Yan'an Formation can be subdivided into two third-order

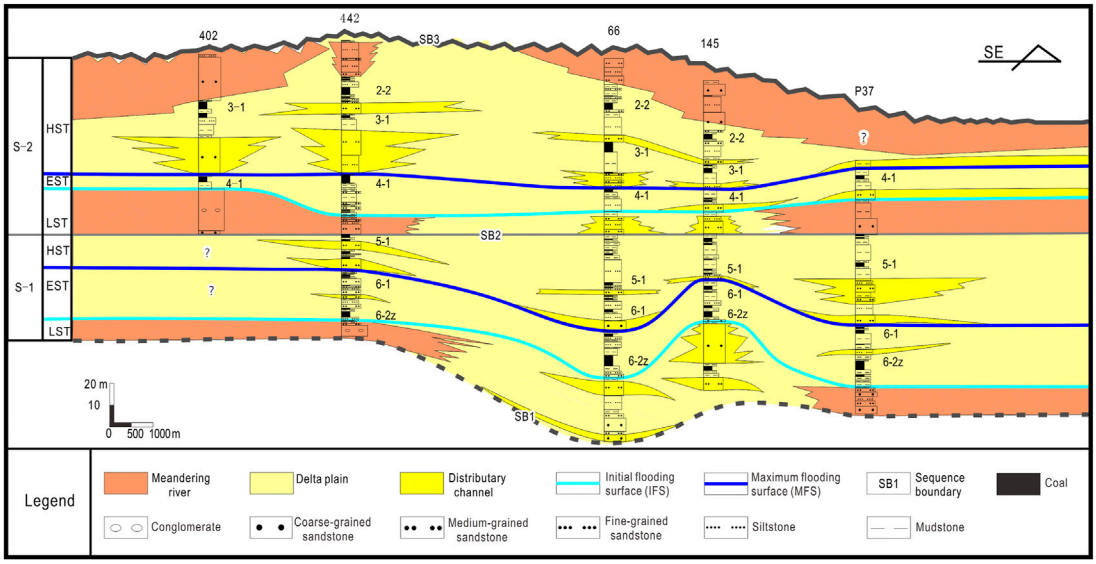

FIGURE 6
NW-SE cross-section (C-C′) through the Yan 'an Formation, showing lithofacies, interpreted depositional environments (including coal seams) and sequence-stratigraphic data. The intraformational sequence boundary SB2 is taken as horizontal. See Figure 1B for location of the cross-section.

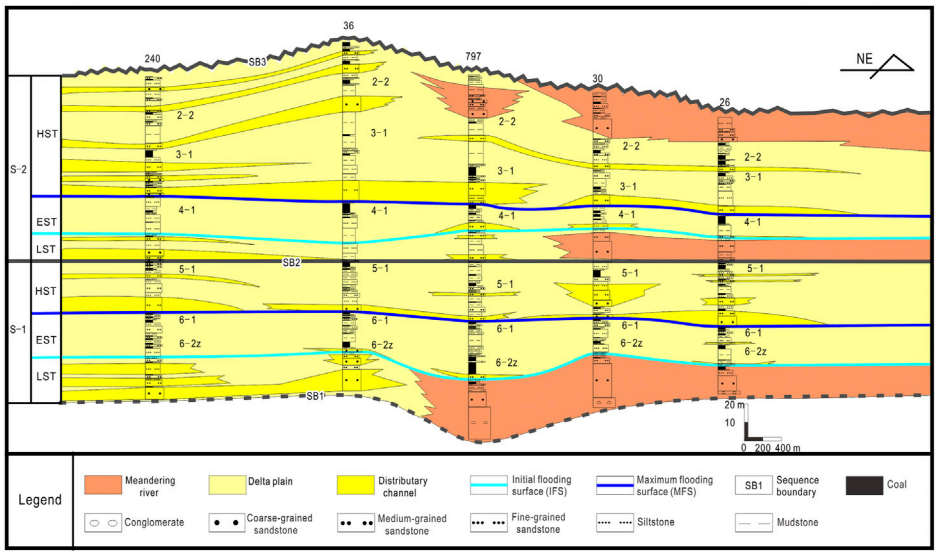

FIGURE 7
NE-SW cross-section (D-D′) through the Yan'an Formation, showing lithofacies, interpreted depositional environments (including coal seams) and sequence-stratigraphic data. The intraformational sequence boundary SB2 is taken as horizontal. See Figure 1B for location of the cross-section.

sequences: S-1 and S-2 (Figures 2, 3). The system tracts were identified by the key surfaces and the sedimentary stacking patterns (Catuneanu, 2002; Catuneanu, 2020), including the lowstand systems tract (LST), extended (lake) system tract (EST), and highstand system tract (HST).

4.2.3.1 *Sequence S-1*

S-1 consists of the sediments between sequence boundaries SB1 and SB2 (Figures 2, 3). It thins from the center of the basin toward all its margins (Figures 4–8) and formed in a meandering river and a lacustrine delta.

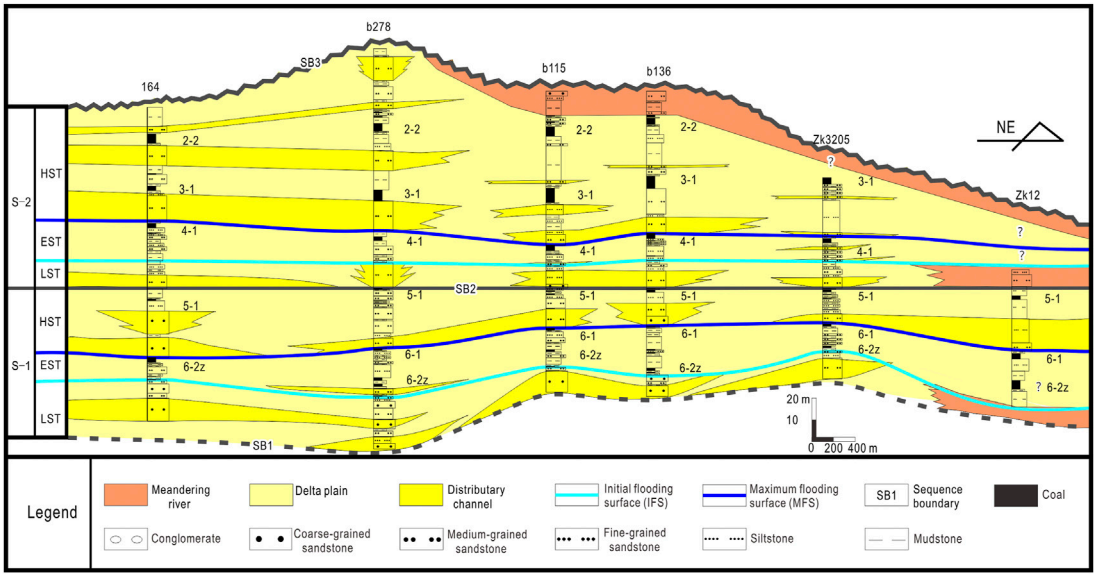

FIGURE 8
NE-SW cross-section (E-E′) through the Yan'an Formation, showing lithofacies, interpreted depositional environments (including coal seams) and sequence-stratigraphic data. The intraformational sequence boundary SB2 is taken as horizontal. See Figure 1B for location of the cross-section.

The LST comprises FA1 and FA2 (mainly lithofacies Gp, St, and Sp), showing a stacking pattern reflecting progradation. A meandering river was situated near the source area and a lacustrine delta was present at the margin of the basin. The EST consists predominantly of FA2 (lithofacies Sr, Sh and FI), reflecting a retrogradation pattern and representing a lacustrine delta. The thickness of the coal seam in the EST, which represents the main coal-forming phase of the Yan'an Formation, is 3–5 m. The HST is composed near the provenance area mainly of FA2 (lithofacies St and Sr, and near the basin of lithofacies FI and Sh). The thickness of the coal seam is 2–3 m. The lake level fell, and the sediments were deposited in a meandering river and on a lacustrine delta (Figures 4–8).

The interpretation of this sequence is that the Yan'an Formation initially (during the LST) inherited the mainly fluvial sedimentary pattern of the Yanchang Formation (Liu et al., 2021). The source area was situated to the north and northwest of the basin. Still during the LST, and continuing during the HST, the supply of clastics from the source area increased and the river channel became extended. Due to the limited accommodation space, no thick coal seams could develop during the LST.

The EST formed during ongoing expansion of the lake area, accompanied by a rise of the base level. The sedimentary environment changed from a meandering river to a lacustrine delta and FA1 became replaced by FA2. Along the margin of the basin, lithofacies FI developed, while a condensed mudstone (MFS) represents the EST in the basin center. The increasing accommodation space kept more or less space with the higher peat production during the EST, so that thick coal seams could develop.

During the HST, the base level was lowered, and clastics were continuously supplied to the basin, resulting in progradation. Although the lake level fell, the accommodation space was initially in balance with the peat production, resulting in a thick coal seam. In a later phase of the HST, the accommodation space was no longer in balance with the possible peat production, so that no thick coal seams developed (Diessel et al., 2000a). The environment consisted for most part of a lacustrine delta, whereas the meandering river remained present only directly adjacent to the source area.

4.2.3.2 *Sequence S-2*

Sequence S-2 is the succession between SB2 at its base and SB3 at its top (Figures 2, 3). It thins from southwest to northeast (Figures 4–8), and it was deposited by a meandering river and a lacustrine delta.

The LST, which consists of FA1 and FA2 (lithofacies St and Sr) and shows progradation characteristics, is thinner than in S-1. A meandering river was present close to the source area, whereas the lacustrine delta was far away. The EST, which is built by FA2 (lithofacies Sr, Sh, Fm, and C; the coal seam is 3 m thick) reflects retrogradation of the lacustrine delta. The HST consists of FA1 and FA2 (lithofacies St, Sr, and FI) with a thick coal seam during the beginning of the HST, and a thin one during a later phase. The HST shows an overall progradation of the delta. Both the meandering river and the lacustrine delta remained the main sedimentary environments (Figures 4–8).

The interpretation of this sequence is that an unconformity with an erosional channel forms the base of this sequence (Supplementary Figure S3C). The lake shrank and the base level of the meandering river near the source area, relatively far away from the lacustrine delta, was lowered. Due to the continuous supply of sediment, the delta became wider, and due to the small accommodation space, no thick coal seams could develop during the LST (Diessel et al., 2000b; Liu et al., 2020).

At the top of the LST, the lake basin expanded and an EST formed with fine-grained sediments. The base level rose and the accommodation space increased, which favored the formation of thick coal seams.

The subsequent HST is represented by a thick succession that consists of lithofacies St, Sr, Sh, and C, and which shows a stacking pattern indicating progradation. Although the base level of the HST was lowered, the accommodation space could initially keep pace with the peat production due to ongoing subsidence, resulting in thick coal seams. Afterwards, a decrease in the subsidence rate caused that the accommodation space was insufficient during the HST for peat accumulation, so that thick coal seams could not develop.

The overall paleogeography did not change fundamentally: a meandering river existed near the source area and a lacustrine delta dominated the margin of the basin.

4.3 Coal petrology

The various aspects mentioned in the methods section about the coal-petrology analysis are dealt with here in the same order: first the results of the maceral analysis (Section 4.3.1), then the TPI and GI indices (Section 4.3.2).

4.3.1 Maceral analysis

Inertinite is the most abundant maceral group with a content varying from 29.85% to 73.22% by volume (Table 3). The content decreases initially upwards, but then increases again (Figure 9A). The vitrinite content varies from 20.06% to 64.29% by volume (Table 3); it increases initially upwards, but then decreases again (Figure 9A). The vitrinite content is lowest in coal seam 6-2z, and maximum in seam 4-1. The liptinite content varies from 2.47% to 9.45% by volume.

The mineral content in the coals varies from 1.45% to 4.05% by volume (Table 3). Like the liptinite, the mineral content is relatively low and relatively stable.

4.3.2 The TPI and GI indices

The GI value, which varies from 0.23 to 9.24, increases initially and then decreases upwards (Supplementary Table S1). This index is relatively high for the 4-1 coal seam. GI indices higher than 1 are found for coal seams 6-1, 5-1, 4-1, and 3-1 coal. These >1 values indicate relatively humid conditions.

TABLE 3 Average maceral and mineral content of the various coal seams in the Yan'an Formation in the study area.

Coal seam	V (vol/%)	I (vol/%)	L (vol/%)	M (vol/%)
2-2	36.57	49.92	9.45	4.05
3-1	47.94	46.03	3.48	2.56
4-1	64.29	29.85	3.14	2.72
5-1	56.38	39.43	2.74	1.45
6-1	39.11	54.75	3.20	2.94
6-2z	20.06	73.22	2.86	3.86

V, vitrinite; I, inertinite; L, liptinite; M, mineral particles.

The TPI values vary from .32 to 9.35 and are mostly higher than 1 (Supplementary Table S1), indicating that the plant tissues are well-preserved and that xylophytes form a major part.

4.4 Relationship between facies and coal development

The above findings indicate that the coal seams in the Yan'an Formation have different characteristics in facies associations FA1 and FA2. Those in FA1 are mostly developed in successions representing an LST or HST, which implies development in a fluvial environment. In contrast, the coal seams in FA2 were formed during the EST in a lacustrine delta environment.

Another difference between FA1 and FA2 regards the thicknesses and petrographic characteristics of the coal seams. Those formed in FA1 are thinner than those in FA2. Moreover, the vitrinite content of the coal in FA1 is lower than in FA2.

The values of the TPI and GI indices in the coals of FA1 are relatively low (TPI < 2 and GI < 1) than those in FA2 (TPI >2 and GI >1) (Figure 9B).

5 Discussion

Several aspects need some more attention. These regard the more precise environment in which the coal seams could develop (Section 5.1) and the factors that controlled the coal development (Section 5.2). On the basis of these analyses, a model for the coal accumulation is developed (Section 5.3).

5.1 Coal-forming environments

The 2-2 coal seam, which is present in FA2, formed during the HST in a meandering river or lacustrine delta environment (Figures 4–8). This occurred when the lake level fell and the accommodation space increased less than the peat production, so

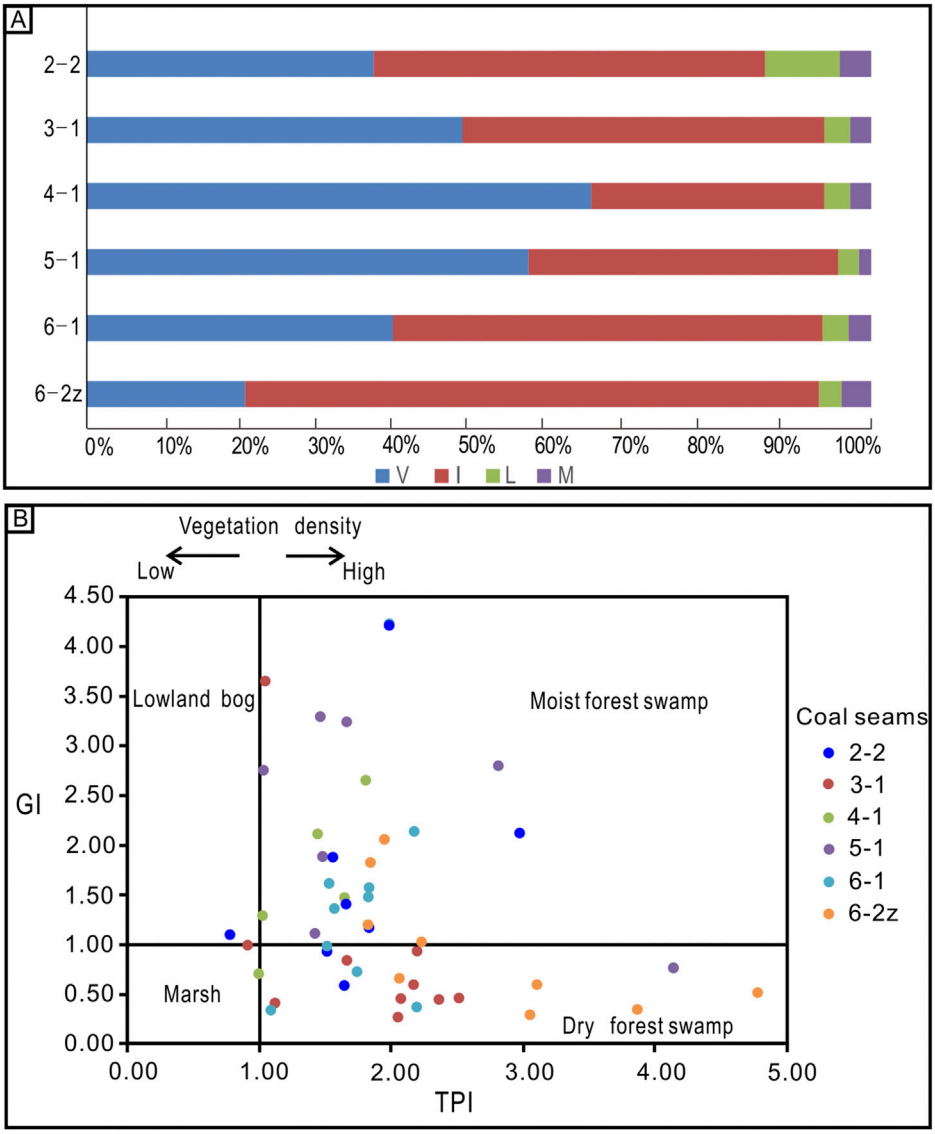

FIGURE 9
(A) Average maceral and mineral content (in weight percentage) of the samples from the six investigated coal seams. V, vitrinite; I, inertinite; L, liptinite; M, mineral particles). **(B)** Relationship between the GI and TPI indices of the coal samples, with environmental interpretation.

that the conditions were not favorable for the development of peat accumulation (Diessel et al., 2000a; Diessel et al., 2000b; Chalmers et al., 2013).

Coal seams 6-2z, 6-1, 5-1, 4-1, and 3-1, which also form part of FA2, occur in the EST or an early phase of the HST; they developed in a lacustrine deltaic environment. There was less supply of clastic sediment, but the accommodation space increased (Figures 4–8). The lake level kept pace with the accommodation space and the peat production. The plant material accumulated during a fairly long time-span, resulting in a thick accumulation of the peat that eventually formed fairly thick coal seams (Diessel et al., 2000a; Diessel et al., 2000b; Chalmers et al., 2013).

As already mentioned in Section 3.3, the TPI and GI indices of the coal samples (Figure 9B) provide additional environmental information, particularly if their mutual relationship is taken into account (Figure 9A). It can thus be deduced that a moist forest swamp existed in which the 6-1, 5-1, 4-1, and 3-1 coal seams were formed, whereas a dry forest swamp enabled the development of the 2-2 and 6-2z coal seams. The environment was thus dominated by a forest peat swamp throughout the peat development (Guatame and Rincón, 2021).

TABLE 4 Tendency (increasing or decreasing) of the maceral characteristics in the coal seams under study.

Coal seam	Coal seam		Coal seam		Coal seam		Coal seam		Coal seam		Coal seam	
	6-2z		6-1		5-1		4-1		3-1		2-2	
	Bottom part	Top part	Bottom part	Top part	Bottom part	Top part	Bottom part	Top part	Bottom part	Top part	Bottom part	Top part
Vitrinite content	↓	↑	↓	↑	↓	↓	↓	↑	↓	↓	↑	↓
Inertinite content	↑	↓	↑	↓	↑	↑	↑	↓	↑	↑	↓	↑
V/I ratio	↓	↑	↓	↑	↓	↓	↓	↑	↓	↓	↑	↓
GI	↓	↑	↓	↑	↓	↓	↓	↑	↓	↑	↑	↓
TPI	↑	↓	↑	↓	↓	↑	↓	↑	↓	↑	↑	↓
AR/PPR	↓	↑	↑	↑	↓	↓	↓	↑	↓	↓	↓	↓
Paleoclimate	Dry	Wet	Dry	Wet	Wet	Dry	Wet	Humid	Wet	Dry	Wet	Dry
Depositional stage	Expansion lake		Expansion lake		Shrinking lake		Expanding lake		Shrinking lake		Shrinking lake	

5.2 Factors controlling coal formation in the study area

Four factors (climate, sediment supply, tectonics and eustasy) tend to control sequence stratigraphy (Holz et al., 2002). In contrast to full-marine basins that are controlled particularly by tectonics and glacially-induced eustasy (Wilgus et al., 1988), the sequence stratigraphy of continental basins is determined primarily by lake-level fluctuations, sediment supply and climate (Petersen et al., 2013; Guo et al., 2018). These are not mutually independent factors, however: sediment supply is largely controlled by climate and tectonics, because they influence weathering, erosion and accommodation space (Holz et al., 2002). Consequently, climate may be considered as a factor that may considerably influence the sequence stratigraphy of stable continental basins (Calder, 1994). The study area was located in the northeastern margin of the Ordos Basin (Zhao et al., 2020), which had a tectonically quiet setting during the Middle Jurassic (Cheng et al., 1997; Li et al., 2015; Zhang et al., 2021a). It is therefore deduced in modern Chinese studies that the most important factor that controlled the coal formation in the succession under study was climate. This is particularly of interest because the characteristics of the macerals (vitrinite and inertinite contents, V/I and AR/PPR ratios, GPI and TI indices) in all six coal seams under study show that wet and dry conditions alternate during the accumulation of the peat while the coal seams originated (Table 4). We will show in Section 5.2.2. That–in contrast to what is commonly assumed nowadays—(probably slightly irregular) subsidence of the basin must have been at least equally important as the climate with respect to the development of the coal measures in the Yan'an Formation.

5.2.1 Maceral characteristics in the coal seams and environmental implications

The vitrinite and inertinite contents in coal are commonly used to reconstruct the depositional environment of the vegetation (Diessel et al., 2000a; Diessel et al., 2000b): vitrinite is formed from the roots and leaves of plants in a reducing environment covered with water, whereas inertinite is formed by the roots and leaves of plants under relatively dry oxidizing conditions. A high content of vitrinite in the coal samples under study thus indicates that the conditions were relatively wet, and that accumulation could take place because the accommodation space increased; in contrast, a high inertinite content indicates that the conditions were relatively dry (Guatame and Rincón, 2021). In other words: the ratio between vitrinite and inertinite (V/I ratio) is a proxy for the degree of reducing conditions to which the peat was exposed (Harvey and Dillon, 1985). If V/I is less than 1, the peat is considered to have accumulated in an oxidizing environment.

The ratio between the increase in accommodation space and the peat production (commonly indicated as the AR/PPR ratio) is also an important index to evaluate the depositional conditions (Bohacs and Suter, 1997; Diessel et al., 2000a; Diessel et al., 2000b; Liu et al., 2020; Wang et al., 2020). The V/I ratio and the GI and TPI indices of the various coal seams, as well as the trends of the vitrinite and inertinite, are shown in Figure 9A and Table 4. More details about the characteristics of the macerals in the six coal seams under study are presented in the following subsections.

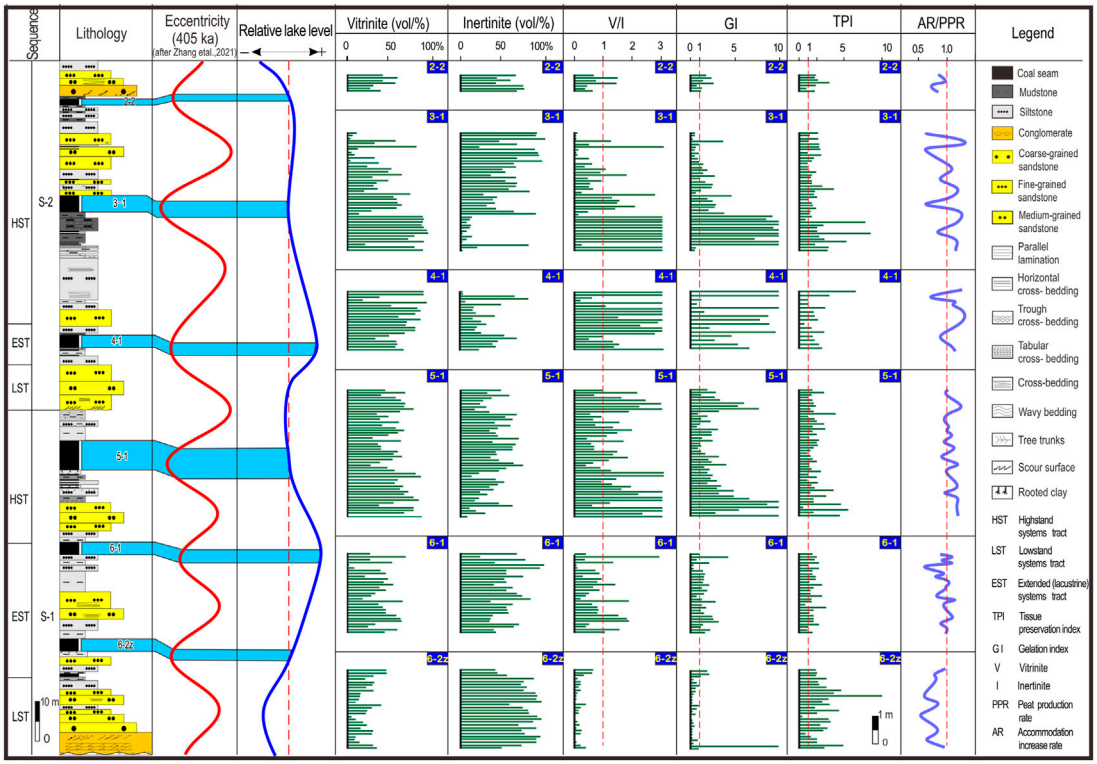

FIGURE 10
Relationship between sequence stratigraphy, occurrences of coal seams, maceral, and the astronomical 405-ka (eccentricity) cycle for the Yan'an Formation in the study area.

5.2.1.1 *Macerals in the 6-2z coal seam*

The vitrinite and inertinite values reflect that the peat accumulated initially in a dry oxidizing environment that changed into a wet reducing environment. The GI and TPI indices reflect that xylophytes dominated and support the finding that the environment changed from dry to wet. The change in the AR/PPR ratio indicates the base level was rising, which is consistent with an expanding lake.

Taking all above data together, it can be deduced that the conditions changed from dry to wet, and that the lake expanded (Figure 10).

5.2.1.2 *Macerals in the 6-1 coal seam*

The vitrinite and inertinite concentrations reflect that the peat was exposed initially to dry, oxidizing conditions that changed into wet, reducing conditions (Table 4). The GI and TPI values are above 1, indicating that xylophytes dominated and supporting the finding that the environment changed from dry to wet. The initially decreasing and subsequently rising AR/PPR values fluctuate around 1; they indicate that the base level was rising so that the lake expanded.

Compared with the 6-2z coal seam, the environment was wetter.

5.2.1.3 *Macerals in the 5-1 coal seam*

The vitrinite and inertinite concentrations reflect wet, reducing conditions, with an upward drying tendency (Table 4). The changing TPI and GI values are more than 1, which indicates that xylophytes dominated and that the environment changed from wet to dry. The AR/PPR ratio, fluctuating between 1 and 1.18, increases upwards, reflecting a rising base level due to a lacustrine transgression.

Compared with the 6-1 coal seam, the environment had become dryer, and the lake was shrinking.

5.2.1.4 *Macerals in the 4-1 coal seam*

The vitrinite and inertinite indicate that the peat was exposed to wet, reducing conditions, changing to humid (Table 4). The TPI and GI values indicate that xylophytes dominated. The AR/PPR ratio changed from less than 1 in the lower part of the seam to more than 1 in the upper part, reflecting a base level drop followed by arise, indicating expansion of the lake.

Compared with the 5-1 coal seam, the environment was wetter.

5.2.1.5 *Macerals in the 3-1 coal seam*

In the 3-1 coal seam, the vitrinite and inertinite values, in combination with the V/I ratio that is more than 1 in the lower

part of the seam and more than 1 in the upper part, indicate that the conditions changed from wet and reducing to dry and oxidizing. The TPI and GI indices simultaneously change from more than 1 to less than 1, indicating that xylophytes dominated and supporting the finding that the conditions changed from wet to dry. The AR/PPR ratio varied but fluctuated around 1; it indicates that the base level was lowered, reflecting a drop of the lake level and consequently shrinking of the lake (Table 4).

Compared with the 4-1 and 5-1 coal seams, the conditions of the 3-1 coal seam were dryer than those of the 4-1 coal seam but similar to those of the 5-1 coal seam.

5.2.1.6 *Macerals in the 2-2 coal seam*

In the 2-2 coal seam, the vitrinite and inertinite contents reflect that the peat was exposed to dry, oxidizing conditions. The TPI and GI values indicate that xylophytes dominated and that the conditions changed from wet to dry (Table 4). The AP/PPR ratio, which is less than 1, indicates that the base level gradually became lower.

Compared with the 3-1 coal seam, the environment was drier, and the lake shrank (Figure 10).

5.2.2 Climate as a factor influencing the sequence stratigraphy

As indicated above, the sediment influx and, particularly, the climate conditions and basin subsidence appear to have controlled the lake level, and, consequently, whether the lake expanded or shrank. The influence of the climate is supported by the maceral variation: the coal seams 6-2z, 6-1, and 4-1 formed in the EST of both sequences (Figure 10). The conditions changed from dry to wet during expansion of the lake, which is consistent with EST characteristics. However, the 5-1, 3-1, and 2-2 coal seams formed during the HST of both sequences. The conditions then changed from wet to dry, during shrinking of the lake, which is consistent with HST characteristics. This shows that the fluctuating lake level was the main factor controlling the sequence stratigraphy, and this must have played an important role in the coal formation. Possibly the fluctuations in the lake level were influenced to some degree by climate changes (resulting in e.g., more or less precipitation and consequently more or less inflow of water, more or less evaporation, etc.), but it is physically impossible that the changing meteorological conditions caused the development of the entire succession of the Yan'an coal measures.

Nevertheless, Liu and Li (2007) proposed that the climate was the main factor to control short-lived sequences without sedimentary hiatuses during tectonically quiet stages of lacustrine environments. However, Zhang et al. (2020) have found that astronomical forcing determined the development of a Paleogene coal-bearing succession, and deduced that climate was the controlling factor of these coal-bearing successions. Moreover, Zhang et al. (2021a) found that the coal of the Yan'an Formation developed during time-spans of eccentricity minima in the 405-ka cycle (Figure 10), whereas eccentricity maxima in these cycles are characterized by detrital sedimentation. During phases of large eccentricity, the differences between seasons are large, which, according to Zhang et al. (2021b), would result in increased river discharge and sediment supply, even though this is not supported by actual data. Moreover, phases of limited eccentricity would, gain according to Zhang et al. (2021a), result in limited seasonal differences and in a stable climate, much vegetation, and reduced sediment supply, whereas the maximum long eccentricity would commonly have been accompanied by a short phase of intensive rainfall and a perennial drought climate, with significant seasonal differences. The time-span of long eccentricity minima must, following Zhang et al. (2021b) usually have been warm and humid, with moderate seasonal variation, which favored vegetation growth and thus was suitable for peat accumulation. Zhang et al. (2021a) therefore consider it likely that the climate influenced the sequence development of the Yan'an coal measures as well as the coal formation. Unfortunately, however, they do not pay attention to the process that must have created sufficient accommodation space for the entire coal-measures succession.

5.2.3 The controlling role of basin subsidence

Ever since astronomical factors have been found to affect sedimentation on Earth, numerous studies (Berger et al., 1992; Liu and Li, 2007; Fang et al., 2017; Huang et al., 2020; Zhang et al., 2020; Zhang et al., 2021b; Huang et al., 2021; Zhao et al., 2022) emphasize the role of astronomically-induced climate changes on the development of specific successions, including coal measures of different ages and in different parts of the world (Cecil et al., 1985; Cecil, 1990; Fielding and Webb, 1996; Miller and Eriksson, 1999; Pashin and Gastaldo, 2004; Izart et al., 2005; Liu and Li, 2007; Falahatkhah et al., 2021; Zainal Abidin et al., 2022). This is remarkable since another factor, *viz.*, basin subsidence, tends to be completely overlooked, even though the successions could not have developed without such subsidence. The Yan'an Formation in the study area is some 170 m thick, and the succession with the coals seams is some 130 m thick. A geologically simple question is how such a lacustrine succession can develop, particularly if the occurrences of coal seams indicate that the entire succession was deposited at roughly the lake level. The answer is just as simple as the question: accommodation space must have been created that allowed sediment to accumulate, eventually reaching a total thickness of at least the succession with the coal seams. This, in turn, raises the simple question of how such an accommodation space can be created within in and along the marginal part of a huge lake. Also, this question has a simple answer: the accumulation of the sediments must have kept roughly pace with the local subsidence of the lake bottom.

This seems, however, not self-evident, as Chinese literature mentions that the Ordos Basin was (apart from some adjacent areas) tectonically quiet and stable during the Mesozoic (Liu and Li, 2007). This commonly accepted view has, unfortunately, led to the unjustified idea that no tectonic activity (such as subsidence) took place. This is the more remarkable since at least four tectonic phases influenced the evolution of the Ordos Basin, or at least the adjacent areas, during the Mesozoic, *viz.*, the Late Triassic Indosinian Orogeny, and the Yanshan I (Early Jurassic), Yanshan II (Late Jurassic) and Yanshan III (Early Cretaceous) phases of the Yanshan cycle.

In spite of the above considerations, it seems scientifically only appropriate to check whether other processes may have resulted in a succession of over 100 m thick with several coal seams. It has been advocated (Liu and Li, 2007) that climate change must have been the main factor that controlled the development (see also Section 5.2.2). The accumulation of clastic sediment with peat on top is then ascribed to a rising lake level under the influence of climate (high precipitation rate, much inflow of river water). This poses several problems, however: where did the precipitation and inflowing water come from? Considering the paleogeographic situation (almost), all this water must have been derived from evaporated water from the Ordos Lake, which implies that the influence on the lake level was negligible and certainly not enough to create an accommodation space for many meters of sediment. A second problem is that the inflow of huge amounts of water from another water source might, indeed, raise the lake level (though only in a very limited way) so that clastic sediments with peat on top could develop, but that a next lake-level drop (as reflected by the sequence stratigraphical characteristics) would have resulted in erosion of the subaerially exposed peat, so that no coal layer would be formed.

Particularly considering the fact that several coal seams are present in a succession of over a hundred meters thick, it must be deduced that the characteristics of the coal measures, in combination with their geological context, falsify the commonly adhered to hypothesis that climate was the main factor controlling the development of the coal measures. On the other hand, it can be deduced that the basin subsidence, which had taken place already for a long time considering the thicknesses of the Triassic formations in the basin, created the accommodation space in which the coal measures could develop. The subsidence, although quiet and continuous if considered over longer time-spans, may have taken place with small irregularities (steps), which might explain the alternating dry and wet conditions under which the plants grew: slow subsidence could easily result in gradually drier conditions because the sedimentation was faster than the subsidence; when quick subsidence occurred, for instance due to small-scale faulting in the subsoil, lowering of the sedimentary surface resulted in a relative rise of the lake level, and consequently in wetter conditions.

Obviously, basin subsidence and climate change can have acted simultaneously, without leaving traces that prove which process prevailed. It should be realized, however, that only subsidence of the lake bottom could create the conditions in which the Yan'an Formation could develop, and under which successive coal seams could be formed.

5.3 Coal-forming model

Many coal-forming models have been presented in the past decade (Wang et al., 2011; Lv et al., 2017; Li et al., 2018; Lv et al., 2019; Li et al., 2020; Wang et al., 2020; Li et al., 2021a; Li et al., 2021b). Most of these models focused on the depositional process, neglecting the role of climate and accommodation space. The model proposed here takes the role of the climate as a factor to control the sequence stratigraphy into account, as well as the role of subsidence as the main factor responsible for the creation of sufficient accommodation space (Figure 11). The model explains the development of the investigated succession with its coal seams but is considered to be equally applicable to other coal measures formed under comparable conditions.

The climate prevailing during an LST was dry, with relatively little rainfall and a relatively low lake level (Figure 11A). There were distinct seasonal differences. The subsidence velocity (Vs) was much higher than the velocity of the lake-level rise (Vr). Along the meandering river, which was the main depositional environment, some vegetations was present, but little of the peat that might be formed could be preserved because of erosion. Consequently, hardly any coal is present in sediments accumulated during an LST.

The beginning of an EST coincided, following Zhang et al. (2021), with a relatively low eccentricity of the orbit of the Earth, resulting in a climate that became wetter, with more rainfall and more vegetation. Simultaneously, a relative rise of the lake level (with velocity Vr) occurred as a result of subsidence of the lake bottom (with velocity Vs). Because Vs was more or less equal to Vr, extensive coal accumulation in the form of the 6-2z coal seam took place at the beginning of the EST (Figure 11B). With increasing eccentricity, the climate was no longer suitable for plant development because of large seasonal differences that caused extensive erosion and sediment removal because Vs was lower than Vr (Figure 11C). When the eccentricity started to decrease again, more and more plants started to develop. The AR/PPR ratio tended toward 1, and coal seams 6-1 and 4-1 developed in the middle and upper stages of the EST (Figure 11D). Subsequently, the AR/PPR ratio rose to over 1 indicating that the climate became wetter; the peatland became covered by water due to the relative rise of the lake level under the influence of ongoing subsidence.

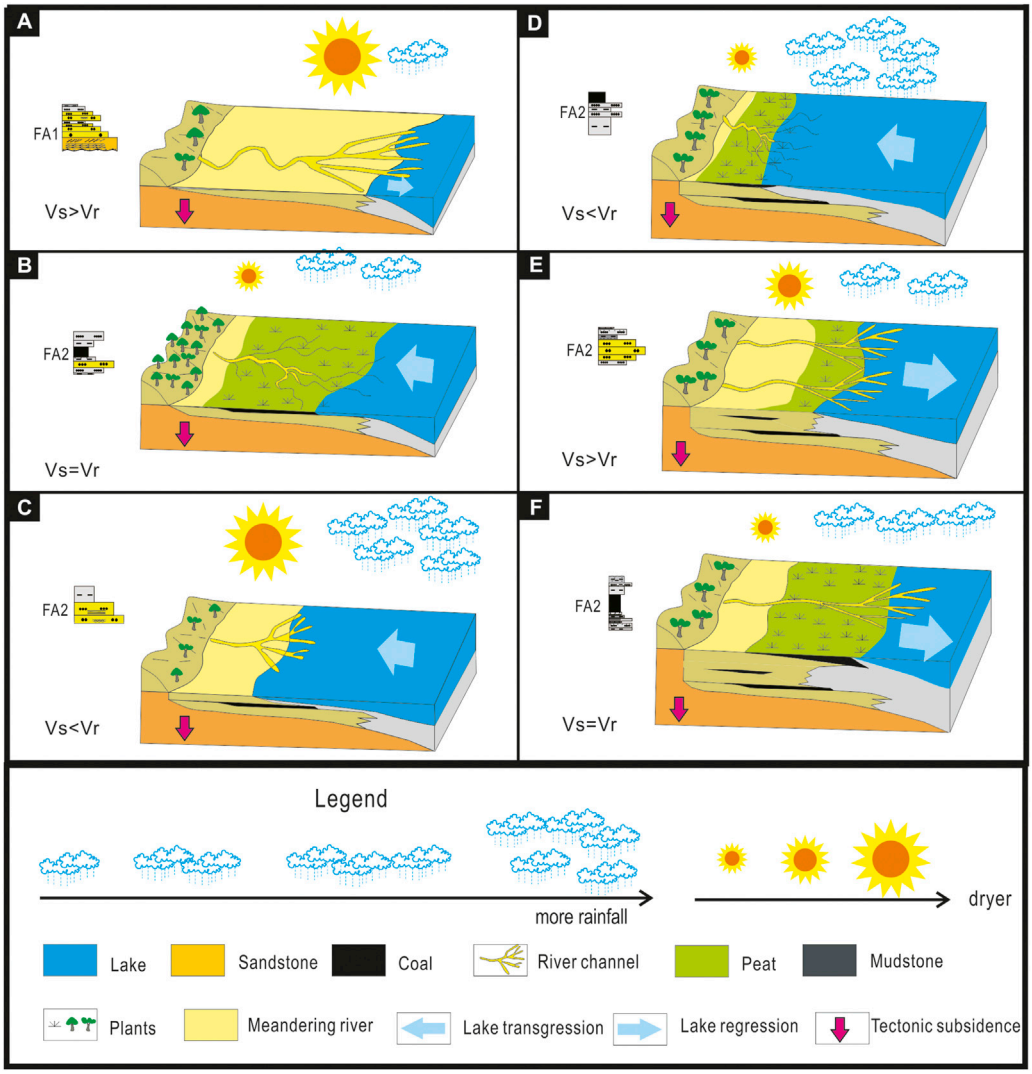

FIGURE 11
Model showing the development of the coal measures in the Yan'an Formation in a fluvial and (lacustrine) deltaic environment, as a consequence of the simultaneous effects of eccentricity-influenced climate change and basin subsidence. Vs = subsidence velocity, Vr = lake-level rise

The climate changed again during the HST because of an increased eccentricity of the Earth's orbit (Figure 11E), resulting in more erosion because the lake level fell and earlier deposited clastic sediments and peat became exposed and were partly eroded. During the stage of the relatively low eccentricity, the supply of clastics was limited (Zhang et al., 2021b). More and more wetlands were formed, resulting in extensive peat areas (the parent material of the 5-1, 3-1, and 2-2 coal seams) where the AR/PPR ratio changed toward (Figure 11F). Increasingly more clastics became supplied by the meandering river, eventually the peats, so that their growth stopped, and the AR/PPR ratio became less than 1.

The coal-bearing cycles in the Yan'an Formation show similar sedimentary characteristics (vertical changes in, depositional conditions, coal distribution, etc.) (Wang et al., 2011; Ielpi, 2012; Lv et al., 2019; Zhang et al., 2021b; Wang et al., 2022), but these characteristics were not yet well explained. The coal-forming model presented here, with the interaction between basin subsidence and climate changes (Zainal Abidin et al., 2022), which sometimes strengthened each other but sometimes reduced the joint effect, explains the lateral distribution and the vertical occurrences of the coal seams in a context of sequence stratigraphy that is at least partly determined by astronomical factors, in particularly the fluctuations in eccentricity of the Earth's orbit.

Consequently, the present study may help deepen the understanding of coal formation, but may equally have a practical significance regarding the exploitation of coals in lacustrine basins. Recycling and regeneration performance.

6 Conclusion

(1) The coal-bearing succession of the Yan'an Formation in the Ordos Basin comprises nine lithofacies, which can be grouped into two lithofacies associations (FA1 and FA2). FA1 was formed in and along a meandering river, whereas FA2 was formed on a lacustrine delta.

(2) Two sequences (S-1 and S-2) are present, bounded by three sequence boundaries (SB1, SB2 and SB3). Each sequence includes three system tracts (LST, EST, and HST). The successions formed during an LST consist of both FA1 and FA2. The EST successions consist of FA2. The successions formed during an HST consist mostly of FA2, but partly of FA1.

(3) The coal seams originated mostly during early stages of an EST or HST, in a delta plain environment. The coal seams 6-2z, 6-1, 5-1, 4-1, and 3-1 forming part of FA2 are thicker than coal seam 2-2 forming part of FA1 because of the longer time-span with sufficient accommodation space during the peat production. The TPI and GI indices in the coals of FA1 are relatively low (TPI l < 2 and GI < 1), whereas those of the coal in FA2 are relatively high (TPI > 2 and GI > 1). The variations of the macerals in the coal seams indicate that the climate controlled the dominant vegetation type and consequently the coal petrology.

(4) In contrast to previous studies, the present contribution shows that the development of coal measures cannot be ascribed exclusively to climate changes, but that basin subsidence must have created the required accommodation space. The (probably irregular but relatively small) basin subsidence interacted with climate change; the joint effect was sometimes relatively large, sometimes smaller, depending on the precise conditions that depended on the sequence stratigraphic development, which, in turn, was influenced by astronomical factors, in particularly the eccentricity of the Earth's orbit.

Data availability statement

The original contributions presented in the study are included in the article/Supplementary Material, further inquiries can be directed to the corresponding author.

Author contributions

LD, SY, and ZZ participated in the fieldwork, LD and ZZ drafted the manuscript. AL, MR, and SG prepared the final text and put the material in the context of the Mesozoic Ordos Basin. RZ and WY made the photographs and WD composed the tables. The interpretation of the field data and the conclusions were a result of input from all authors. All authors have read and approved the final manuscript.

Funding

This study was financially supported by the National Key R&D Plan of China (Grant no. 2022YFC2903402), the National Natural Science Foundation of China (Grants nos. 41772096 and 42102127), and the SDUST Research Fund (Grant no. 2018TDJH101).

Acknowledgments

We thank the editors and reviewers for giving us many constructive comments that significantly improved the paper.

Conflict of interest

The authors declare that the research was conducted in the absence of any commercial or financial relationships that could be construed as a potential conflict of interest.

Publisher's note

Supplementary material

The Supplementary Material for this article can be found online at: https://www.frontiersin.org/articles/10.3389/feart.2022.1086298/full#supplementary-material

References

Akhtar, S., Yang, X., and Pirajno, F. (2017). Sandstone type uranium deposits in the ordos Basin, northwest China: A case study and an overview. *J. Asian Earth Sci.* 146, 367–382. doi:10.1016/j.jseaes.2017.05.028

Akinyemi, S. A., Adebayo, O. F., Madukwe, H. Y., Kayode, A. T., Aturamu, A. O., OlaOlorun, O. A., et al. (2022). Elemental geochemistry and organic facies of selected Cretaceous coals from the Benue Trough Basin in Nigeria: Implication for paleodepositional environments. *Mar. Petroleum Geol.* 137, 105490. doi:10.1016/j.marpetgeo.2021.105490

Berger, A., Loutre, M. F., and Laskar, J. (1992). Stability of the astronomical frequencies over the Earth's history for paleoclimate studies. *Science* 255, 560–566. doi:10.1126/science.255.5044.560

Biswas, S., Varma, A. K., Kumar, M., and Saikia, B. K. (2021). Multi-analytical approach of provenance signatures and indication of marine environment in coal and shale bearing sequence from Makum Coalfield, India. *Arab. J. Geosci.* 14, 2183–2223. doi:10.1007/s12517-021-08569-z

Bohacs, K., and Suter, J. (1997). Sequence stratigraphic distribution of coaly rocks: Fundamental controls and paralic examples. *AAPG Bull.* 81, 1612–1639. doi:10.1306/3B05C3FC-172A-11D7-8645000102C1865D

Boyd, R., Dalrymple, R. W., and Zaitlin, B. A. (2006). Estuarine and incised-valley facies models. *Facies Models Revisited, SEPM Spec. Publ. (Tulsa)*. Editors H. W. Posamentier and R. G. Walker 84, 171–234. doi:10.2110/pec.06.84.0171

Calder, J. H. (1994). The impact of climate change, tectonism and hydrology on the formation of carboniferous tropical intermontane mires: The springhill coalfield, cumberland basin, nova scotia. *Palaeogeogr. Palaeoclimatol. Palaeoecol.* 106 (1-4), 323–351. doi:10.1016/0031-0182(94)90017-5

Cameron, A. R., Goodarzi, F., and Potter, J. (1994). Coal and oil shale of early carboniferous age in northern Canada: Significance for paleoenvironmental and paleoclimatic interpretations. *Palaeogeogr. Palaeoclimatol. Palaeoecol.* 106, 135–155. doi:10.1016/0031-0182(94)90007-8

Catuneanu, O., Abreu, V., Bhattacharya, J. P., Blum, M. D., Dalrymple, R. W., Eriksson, P. G., et al. (2009). Towards the standardization of sequence stratigraphy. *Earth-Science Rev.* 92, 1–33. doi:10.1016/j.earscirev.2008.10.003

Catuneanu, O. (2019). Model-independent sequence stratigraphy. *Earth-Science Rev.* 188, 312–388. doi:10.1016/j.earscirev.2018.09.017

Catuneanu, O. (2006). *Principles of sequence stratigraphy*, 388. Elsevier Science.

Catuneanu, O. (2020). Sequence stratigraphy in the context of the 'modeling revolution. *Mar. Petroleum Geol.* 116, 104309. doi:10.1016/j.marpetgeo.2020.104309

Catuneanu, O. (2002). Sequence stratigraphy of clastic systems: Concepts, merits, and pitfalls. *J. Afr. Earth Sci.* 35, 1–43. doi:10.1016/s0899-5362(02)00004-0

Cecil, C. B. (1990). Paleoclimate controls on stratigraphic repetition of chemical and siliciclastic rocks. *Geol.* 18, 533–536. doi:10.1130/0091-7613(1990)018<0533:pcosro>2.3.co;2

Cecil, C. B., Stanton, R. W., Neuzil, S. G., Dulong, F. T., Ruppert, L. F., and Pierce, B. S. (1985). Paleoclimate controls on late Paleozoic sedimentation and peat formation in the central Appalachian Basin (USA). *Int. J. Coal Geol.* 5, 195–230. doi:10.1016/0166-5162(85)90014-x

Chalmers, G. R. L., Boyd, R., and Diessel, C. F. K. (2013). Accommodation-based coal cycles and significant surface correlation of low-accommodation Lower Cretaceous coal seams, Lloydminster heavy oil field, Alberta, Canada: Implications for coal quality distribution. *Am. Assoc. Pet. Geol. Bull.* 97, 1347–1369. doi:10.1306/12181211187

Chen, Z., Li, F., and Zhang, P. (2022). High-resolution terrestrial record of orbital climate forcing in the coal-bearing Middle Jurassic Yan'an Formation, Ordos Basin, north China. *Geol. J.* 57, 1873–1890. doi:10.1002/gj.4385

Cheng, S., Huang, Y., and Fu, X. (1997). Paleogeography reconstruction of the Early-Middle Jurassic large Ordos Basin and development and evolution of continental downwarping. *Acta Sedimentol. Sin.* 15, 43

Dai, S., and Finkelman, R. B. (2018). Coal geology in China: An overview. *Int. Geol. Rev.* 60, 531–534. doi:10.1080/00206814.2017.1405287

Diesel, C. F. K., and Wolff-Fischer, E. (1986). Comparative examinations on coals and cokes in terms of their inertinite reactivity. *Forschungsh.* 47, 203

Diessel, C. F. K., Boyd, R., Wadsworth, J., and Chalmers, G. (2000b). "Significant surfaces and accommodation trends in paralic coal seams," in *Advances in the study of the sydney basin*. Editors R. Boyd, C. F. K. Diessel, and S. Francis, 15–20.

Diessel, C. F. K., Boyd, R., Wadsworth, J., Leckie, D., and Chalmers, G. (2000a). On balanced and unbalanced accommodation/peat accumulation ratios in the Cretaceous coals from Gates Formation, Western Canada, and their sequence-stratigraphic significance. *Int. J. Coal Geol.* 43, 143–186. doi:10.1016/s0166-5162(99)00058-0

Diessel, C. F. K. (1992a). "Coal facies and depositional environment, coal-bearing depositional systems," in *Coal-bearug sepositioal ststems* (Springer (Heidelberg), 161.

Diessel, C. F. K., and Gammidge, L. (1998). Isometamorphic variations in the reflectance and fluorescence of vitrinite - a key to depositional environment. *Int. J. Coal Geol.* 36, 167–222. doi:10.1016/s0166-5162(98)00003-2

Diessel, C. F. K. (1986). *On the correlation between coal facies and depositional environments*. New South Wales: Proceedings 20th Symposium of the Department of Geology, University of New Castle, 19.

Diessel, C. F. K. (1992b). "The conditions of peat formation," in *Coal-bearing depositional systems* (Heidelberg: Springer), 5–39.

Edress, N. A. A., Attia, G. M., and Abdel-Fatah (2021). Construct a paleo-limnological environment based on coal petrography; case study, two selected coal seams, North Crowsnest Open-Pit Mine, Canada. *Iraqi Geol. J.* 54, 1–14. doi:10.46717/igj.54.2d.1ms-2021-10-20

Falahatkhah, O., Kordi, M., Fatemi, V., and Koochi, H. H. (2021). Recognition of milankovitch cycles during the oligocene–early miocene in the zagros basin, SW Iran: Implications for paleoclimate and sequence stratigraphy. *Sediment. Geol.* 421, 105957. doi:10.1016/j.sedgeo.2021.105957

Fang, Q., Wu, H., Hinnov, L. A., Jing, X., Wang, X., Yang, T., et al. (2017). Astronomical cycles of Middle Permian Maokou Formation in South China and their implications for sequence stratigraphy and paleoclimate. *Palaeogeogr. Palaeoclimatol. Palaeoecol.* 474, 130–139. doi:10.1016/j.palaeo.2016.07.037

Fielding, C. R. (2021). Late Palaeozoic cyclothems–A review of their stratigraphy and sedimentology. *Earth-Science Rev.* 217, 103612. doi:10.1016/j.earscirev.2021.103612

Fielding, C. R., and Webb, J. A. (1996). Facies and cyclicity of the late permian bainmedart coal measures in the northern prince charles mountains, MacRobertson land, Antarctica. *Sedimentology* 43, 295–322. doi:10.1046/j.1365-3091.1996.d01-6.x

Flores, D. (2002). Organic facies and depositional palaeoenvironment of lignites from Rio Maior Basin (Portugal). *Int. J. Coal Geol.* 48, 181–195. doi:10.1016/s0166-5162(01)00057-x

Guatame, C., and Rincón, M. (2021). Coal petrology analysis and implications in depositional environments from upper cretaceous to miocene: A study case in the eastern cordillera of Colombia. *Int. J. Coal Sci. Technol.* 8, 869–896. doi:10.1007/s40789-020-00396-z

Guo, B., Shao, L., Hilton, J., Wang, S., and Zhang, L. (2018). Sequence stratigraphic interpretation of peatland evolution in thick coal seams: Examples from yimin formation (early cretaceous), hailaer basin, China. *Int. J. Coal Geol.* 196, 211–231. doi:10.1016/j.coal.2018.07.013

Harvey, R. D., and Dillon, J. W. (1985). Maceral distributions in Illinois coals and their paleoenvironmental implications. *Int. J. Coal Geol.* 5, 141–165. doi:10.1016/0166-5162(85)90012-6

Holz, M., Kalkreuth, W., and Banerjee, I. (2002). Sequence stratigraphy of paralic coal-bearing strata: An overview. *Int. J. Coal Geol.* 48, 147–179. doi:10.1016/s0166-5162(01)00056-8

Huang, H., Gao, Y., Jones, M. M., Tao, H., Carroll, A. R., Ibarra, D. E., et al. (2020). Astronomical forcing of Middle Permian terrestrial climate recorded in a large paleolake in northwestern China. *Palaeogeogr. Palaeoclimatol. Palaeoecol.* 550, 109735. doi:10.1016/j.palaeo.2020.109735

Huang, H., Gao, Y., Ma, C., Niu, L., Dong, T., Cheng, H., et al. (2021). Astronomical constraints on the development of alkaline lake during the carboniferous-permian period in North pangea. *Glob. Planet. Change* 207, 103681. doi:10.1016/j.gloplacha.2021.103681

Hwang, I. G., Chough, S. K., Hong, S. W., and Choe, M. Y. (1995). Controls and evolution of fan delta systems in the miocene pohang basin, SE korea. *Sediment. Geol.* 98, 147–179. doi:10.1016/0037-0738(95)00031-3

ICCP (International (1998). Committee for coal petrology), the new vitrinite classification (ICCP system 1994). *Fuel* 77, 349

Ielpi, A. (2012). Anatomy of major coal successions: Facies analysis and sequence architecture of a Brown coal-bearing valley fill to lacustrine tract (Upper Valdarno Basin, Northern Apennines, Italy). *Sediment. Geol.* 265/266, 163–181. doi:10.1016/j.sedgeo.2012.04.006

Izart, A., Palain, C., Malartre, F., Fleck, S., and Michels, R. (2005). Paleoenvironments, paleoclimates and sequences of Westphalian deposits of Lorraine coal basin (Upper Carboniferous, NE France). *Bull. Société géologique Fr.* 176, 301–315. doi:10.2113/176.3.301

Jiao, Y., Wu, L., Rong, H., Peng, Y., Miao, A., and Wang, X. (2016). The relationship between Jurassic coal measures and sandstone-type uranium deposits in the northeastern Ordos Basin, China. *Acta Geol. Sin. - Engl. Ed.* 90, 2117–2132. doi:10.1111/1755-6724.13026

Jiu, B., Huang, W., and Hao, R. (2021). A method for judging depositional environment of coal reservoir based on coal facies parameters and rare Earth element parameters. *J. Petroleum Sci. Eng.* 207, 109128. doi:10.1016/j.petrol.2021.109128

Johnson, E. A., Liu, S., and Zhang, Y. (1989). Depositional environments and tectonic controls on the coal-bearing lower to middle jurassic yan'an Formation, southern Ordos Basin, China. *Geol.* 17, 1123–1126. doi:10.1130/0091-7613(1989)017<1123:deatco>2.3.co;2

Junnila, R. M., and Young, G. M. (1995). The paleoproterozoic upper gowganda formation, whitefish falls area, ontario, Canada: Subaqueous deposits of a braid delta. *Can. J. Earth Sci.* 32, 197–209. doi:10.1139/e95-016

Klein, G. V. (1990). Pennsylvanian time scales and cycle periods. *Geol.* 18, 455–457. doi:10.1130/0091-7613(1990)018<0455:ptsacp>2.3.co;2

Klein, G. V., and Willard, D. A. (1989). Origin of the pennsylvanian coal-bearing cyclothems of north America. *Geol.* 17, 152–155. doi:10.1130/0091-7613(1989)017<0152:ootpcb>2.3.co;2

Kneller, B. C., and Branney, M. J. (1995). Sustained high-density turbidity currents and the deposition of thick massive sands. *Sedimentology* 42, 607–616. doi:10.1111/j.1365-3091.1995.tb00395.x

Krassay, A., Bradshaw, B., Domagala, J., and Jackson, M. (2000). Siliciclastic shoreline to growth-faulted, turbiditic sub-basins: The proterozoic river supersequence of the upper McNamara group on the lawn hill platform, northern Australia. *Aust. J. Earth Sci.* 47, 533–562. doi:10.1046/j.1440-0952.2000.00790.x

Li, S., Cheng, S., Yang, S., Huang, Q., Xie, X., and Jiao, Y. (1992). *Sequence stratigraphy and depositional system analysis of the northeastern Ordos Basin*. Beijing: Geological Publishing House, 100.

Li, Y., Shao, L., Fielding, C. R., Wang, D., Mu, G., and Luo, H. (2020). Sequence stratigraphic analysis of thick coal seams in paralic environments – a case study from the Early Permian Shanxi Formation in the Anhe coalfield, Henan Province, North China. *Int. J. Coal Geol.* 222, 103451. doi:10.1016/j.coal.2020.103451

Li, Y., Shao, L., Fielding, C. R., Wang, D., and Mu, G. (2021a). Sequence stratigraphy, paleogeography, and coal accumulation in a lowland alluvial plain, coastal plain, and shallow-marine setting: Upper Carboniferous–Permian of the Anyang–Hebi coalfield, Henan Province, North China. *Palaeogeogr. Palaeoclimatol. Palaeoecol.* 567, 110287. doi:10.1016/j.palaeo.2021.110287

Li, Y., Shao, L., Hou, H., Tang, Y., Yuan, Y., Zhang, J., et al. (2018). Sequence stratigraphy, palaeogeography, and coal accumulation of the fluvio-lacustrine Middle Jurassic Xishanyao Formation in central segment of southern Junggar Basin, NW China. *Int. J. Coal Geol.* 192, 14–38. doi:10.1016/j.coal.2018.04.003

Li, Y., Wang, Z., Wu, P., and Meng, S. (2021b). Paleoenvironment reconstruction of the upper paleozoic in the linxing area, northeastern Ordos Basin, China. *Am. Assoc. Pet. Geol. Bull.* 105, 2545–2574. doi:10.1306/07022119233

Li, Z., Dong, S., Feng, S., and Qu, H. (2015). Sedimentary response to middle-late jurassic tectonic events in the Ordos Basin. *Acta Geosci. Sin.* 36, 22–30.

Liu, K., Liu, J., and Huang, X. (2021). Coupled stratigraphic and petroleum system modeling: Examples from the Ordos Basin, China. *Am. Assoc. Pet. Geol. Bull.* 105, 1–28. doi:10.1306/0727201612317147

Liu, Z., and Li, S. (2007). Paleoclimatic cycles of depositional record and their control over the formation of high-frequency sequences. *Geol. Sci. Technol. Inf.* 26, 30–34. (in Chinese)

Liu, Z., Wei, Y., Hua, F., Min, F., Jia, X., and Cao, D. (2020). Control of accommodation changes over coal composition: Case study of jurassic medium-thick coal seams in the Ordos Basin, China. *Arabian J. Geosciences* 13, 1–15. doi:10.1007/s12517-020-5205-3

Lowe, D. R. (1982). Sediment gravity flows; II, Depositional models with special reference to the deposits of high-density turbidity currents. *J. Sediment. Res.* 52, 279.

Lu, J., Shao, L., ang, Y. M., Zhou, K., Wheeley, J. R., Wang, H., et al. (2017). Depositional model for peat swamp and coal facies evolution using sedimentology, coal macerals, geochemistry and sequence stratigraphy. *J. Earth Sci.* 28, 1163–1177. doi:10.1007/s12583-016-0942-7

Lv, D., Li, Z., Wang, D., Li, Y., Liu, H., Liu, Y., et al. (2019). Sedimentary model of coal and shale in the Paleogene lijiaya Formation of the huangxian basin: Insight from petrological and geochemical characteristics of coal and shale. *Energy fuels.* 33, 10442–10456. doi:10.1021/acs.energyfuels.9b01299

Lv, D., Wang, D., Li, Z., Liu, H., and Li, Y. (2017). Depositional environment, sequence stratigraphy and sedimentary mineralization mechanism in the coal bed- and oil shale-bearing succession: A case from the Paleogene huangxian basin of China. *J. Petroleum Sci. Eng.* 148, 32–51. doi:10.1016/j.petrol.2016.09.028

Ma, Y., Liu, C., Zhao, J., Huang, L., Yu, L., and Wang, J. (2007). Characteristics of bleaching of sandstone in northeast of Ordos Basin and its relationship with natural gas leakage. *Sci. China Ser. D-Earth. Sci.* 50, 153–164. doi:10.1007/s11430-007-6020-3

Miall, A. D. (1977). A review of the braided-river depositional environment. *Earth-Science Rev.* 13, 1–62. doi:10.1016/0012-8252(77)90055-1

Miall, A. D. (2013). *Principles of sedimentary basin analysis*. New York: Springer Science & Business Media, 668.

Miall, A. D. (1996). *The geology of fluvial deposits - sedimentary facies, basin analysis, and petroleum geology*. Springer (Berlin/Heidelberg, 582.

Miller, D. J., and Eriksson, K. A. (1999). Linked sequence development and global climate change: The upper mississippian record in the appalachian basin. *Geol.* 27, 35–38. doi:10.1130/0091-7613(1999)027<0035:lsdagc>2.3.co;2

Mjos, R., and Prestholm, E. (1993). The geometry and organization of fluviodeltaic channel sandstones in the Jurassic Saltwick Formation, Yorkshire, England. *Sedimentology* 40, 919–935. doi:10.1111/j.1365-3091.1993.tb01369.x

Nemec, W., and Steel, R. J. (1988). *Fan deltas: Sedimentology and tectonic settings*. Glasgow: Blackie and son, 444.

Pashin, J. C., and Gastaldo, R. A. (2004). Sequence stratigraphy, paleoclimate, and tectonics of coal-bearing strata. *AAPG Stud. Geol.* 51, 238.

Petersen, H. I., Lindström, S., Therkelsen, J., and Pedersen, G. K. (2013). Deposition, floral composition and sequence stratigraphy of uppermost Triassic (Rhaetian) coastal coals, southern Sweden. *Int. J. Coal Geol.* 116, 117–134. doi:10.1016/j.coal.2013.07.004

Plint, A. G., McCarthy, P. J., and Faccini, U. F. (2001). Nonmarine sequence stratigraphy: Updip expression of sequence boundaries and systems tracts in a high-resolution framework, cenomanian dunvegan formation, alberta foreland basin, Canada. *AAPG Bull.* 85, 1967–2001. doi:10.1306/8626D0C7-173B-11D7-8645000102C1865D

Reading, H. G. (1996). *Sedimentary environments: Processes, facies and stratigraphy*. 3rd ed. Oxford: Blackwell Science, 689.

Shanley, K. W., and McCabe, P. J. (1994). Perspectives on the sequence stratigraphy of continental strata. *AAPG Bull.* 78, 544

Souza, A. C. B. d., Nascimento, D. R. d., Nepomuceno Filho, F., Batezelli, A., Santos, F. H. d., eopoldino Oliveira, L. K. M., et al. (2021). Sequence stratigraphy and organic geochemistry: An integrated approach to understand the anoxic events and paleoenvironmental evolution of the Ceará Basin, Brazilian equatorial margin. *Mar. Petroleum Geol.* 129, 105074. doi:10.1016/j.marpetgeo.2021.105074

Sýkorová, I., Pickel, W., Christanis, K., Wolf, M., Taylor, G., and Flores, D. (2005). Classification of huminite - ICCP system 1994. *Int. J. Coal Geol.* 62, 85–106. doi:10.1016/j.coal.2004.06.006

Taylor, G. H., Teichmüller, M., Davis, A., Diessel, C. F. K., Littke, R., Robert, R., et al. (1998). *Organic Petrology*. Berlin: Gebrueder Borntraeger, 704.

Teichmüller, M. (1989). The Genesis of coal from the viewpoint of coal petrology. *Int. J. Coal Geol.* 12, 1–87. doi:10.1016/0166-5162(89)90047-5

Van Wagoner, J. C., Posamentier, H., Mitchum, R., Vail, P., Sarg, J., and Loutit, T. (1988). An overview of the fundamentals of sequence stratigraphy and key definitions. *SEPM Spec. Publ.* 42, 39

Wang, H., Shao, L., Hao, L., Zhang, P., Glasspool, I. J., Wheeley, J. R., et al. (2011). Sedimentology and sequence stratigraphy of the Lopingian (Late Permian) coal measures in southwestern China. *Int. J. Coal Geol.* 85, 168–183. doi:10.1016/j.coal.2010.11.003

Wang, L., Lv, D., Hower, J. C., Zhang, Z., Raji, M., Tang, J., et al. (2022). Geochemical characteristics and paleoclimate implication of middle jurassic coal in the Ordos Basin, China. *Ore Geol. Rev.* 144, 104848. doi:10.1016/j.oregeorev.2022.104848

Wang, S., Shao, L., Wang, D., Hilton, J., Guo, B., and Lu, J. (2020). Controls on accumulation of anomalously thick coals: Implications for sequence stratigraphic analysis. *Sedimentology* 67, 991–1013. doi:10.1111/sed.12670

Wang, X., Pan, S., Yang, Q., Hou, S., Jiao, Y., et al. (2018). Occurrence of analcime in the middle jurassic coal from the Dongsheng coalfield, northeastern Ordos Basin, China. *Int. J. Coal Geol.* 196, 126–138. doi:10.1016/j.coal.2018.07.004

Ward, C. R. (1984). *Coal geology and coal Technology*. Blackwell Scientific Publications, 345.

Wescott, W. A., and Ethridge, F. G. (1980). Fan-delta sedimentology and tectonic setting - yallahs Fan Delta, southeast Jamaica1. *AAPG Bull.* 64, 374–399.

Wilgus, C. K., Hastings, B. S., Posamentier, H., an Wagoner, V. J., Ross, C. A., and Kendall, C. G. S. C. (1988). *sea-level changes: An integrated approach*, 42. SEPM Special Publication, 155

R. Yang and A. J. Van Loon (Editors) (2022). *The Ordos Basin – sedimentological research for hydrocarbons exploration* (Amsterdam: Elsevier), 514.

Yao, J., Deng, X., Zhao, Y., Han, T., Chu, M., and Pang, J. (2013). Characteristics of tight oil in triassic Yanchang Formation, Ordos Basin. *Petroleum Explor. Dev.* 40, 161–169. doi:10.1016/s1876-3804(13)60019-1

Zainal Abidin, N. S., Mustapha, K. A., Abdullah, W. H., and Konjing, Z. (2022). Paleoenvironment reconstruction and peat-forming conditions of Neogene paralic coal sequences from Mukah, Sarawak, Malaysia. *Sci. Rep.* 12, 8870–8926. doi:10.1038/s41598-022-12668-6

Zhang, J., Pas, D., Krijgsman, W., Wei, W., Du, X., Zhang, C., et al. (2020). Astronomical forcing of the Paleogene coal-bearing hydrocarbon source rocks of the east China sea shelf basin. *Sediment. Geol.* 406, 105715. doi:10.1016/j.sedgeo.2020.105715

Zhang, L., Liu, C., Fayek, M., Wu, B., Lei, K., Cun, X., et al. (2017). Hydrothermal mineralization in the sandstone–hosted Hangjinqi uranium deposit, north Ordos Basin, China. *Ore Geol. Rev.* 80, 103–115. doi:10.1016/j.oregeorev.2016.06.012

Zhang, L., Liu, C., Zhang, S., Fayek, M., Lei, K., and Quan, X. (2022). Unconformity-controlled bleaching of jurassic-triassic sandstones in the Ordos Basin, China. *J. Petroleum Sci. Eng.* 211 (2022), 110154. doi:10.1016/j.petrol.2022.110154

Zhang, Q., Li, W., and Liu, W. (2021). Jurassic sedimentary system and paleogeographic evolution of Ordos Basin. *Chin. J. Geol.* 56, 1106–1119. (in Chinese)

Zhang, Q., Liu, Y., Wang, B., Ruan, J., Yn, an, Chen, H., et al. (2022b). Effects of pore-throat structures on the fluid mobility in Chang 7 tight sandstone reservoirs of Longdong area, Ordos Basin. *Mar. Petroleum Geol.* 135, 105407. doi:10.1016/j.marpetgeo.2021.105407

Zhang, Z., Wang, T., Ramezani, J., Lv, D., and Wang, C. (2021). Climate forcing of terrestrial carbon sink during the Middle Jurassic greenhouse climate: Chronostratigraphic analysis of the Yan'an Formation, Ordos Basin, north China. *GSA Bull.* 133, 1723–1733. doi:10.1130/b35765.1

Zhao, J., Liu, C., Huang, L., Zhang, D., and Wang, D. (2020). Paleogeography reconstruction of a multi-stage modified intra-cratonic basin—A case study from the jurassic Ordos Basin, Western north China craton. *J. Asian Earth Sci.* 190, 104191. doi:10.1016/j.jseaes.2019.104191

Zhao, J., Liu, C., Wang, X., Zhang, C., and Van Loon, A. J. (2022). "Subsidence of the mesozoic Ordos Basin and resulting migration of depocenters," in *The Ordos Basin –sedimentological research for hydrocarbons exploration*. Editors R. Yang and A. J. Van Loon (Amsterdam: Elsevier), 153